Generalised non-dimensional multi-parametric involute spur gear design model considering manufacturability and geometrical compatibility

Amani, Amin; Spitas, Christos; Spitas, Vasilios

DOI
10.1016/j.mechmachtheory.2016.11.012

Publication date
2017

Document Version
Final published version

Published in
Mechanism and Machine Theory

Mechanism and Machine Theory 109 (2017) 250–277

Contents lists available at ScienceDirect

Mechanism and Machine Theory

journal homepage: www.elsevier.com/locate/mechmachtheory

Generalised non-dimensional multi-parametric involute spur gear design model considering manufacturability and geometrical compatibility

A. Amani[a], C. Spitas[a,b,*], V. Spitas[c]

[a] Faculty of Industrial Design Engineering, Delft University of Technology, Landbergstraat 15, 2628CE Delft, Netherlands
[b] School of Engineering, Nazarbayev University, Kazakhstan
[c] School of Mechanical Engineering, National Technical University of Athens, Greece

ARTICLE INFO

Keywords:
Spur gears
Addendum
Dedendum
Cutter tip radius
Tooth thickness
Pressure angle
Interference
Corner contact
Tooth pointing
Undercutting
Non-standard
Non-dimensional
Design guideline

ABSTRACT

A generalised non-dimensional multi-parametric model for involute spur gear design is presented, considering manufacturability and geometrical compatibility, where the latter considers various modes of interference and accounts for the combined effects of the module, pressure angle, tooth addendum, dedendum, cutter tip radius, and the numbers of teeth of a pair of mating gears. The effect of the same parameters together with tooth thickness on the manufacturability of the individual gear teeth is also modelled in terms of pointing and undercutting. The full range of parameter values, including non-standard ones, is considered. The resulting combined model serves to provide a complete analytical overview of the multi-parametric design space and is suitable for the fast assessment of existing designs, for implicit or explicit (direct) gear design, for extracting design guidelines, and for design optimisation. The model can be used to identify and explore highly promising under-used subspaces of the parametric design space, which are currently of significant interest to i.e. the automotive and aerospace industries.

1. Introduction

1.1. General framing of the problem

In almost all kinds of industrial applications for motion and power transmission such as automotive, aerospace, robotics, machinery etc., gears - and involute gears in particular- are indispensable and mission critical elements of the design. Gear design itself is a complex process that, in spite of much accumulated knowledge and supporting standards, computational models [1–7] and software [8–12], still critically depends on the experience of the designer, especially if time constraints prohibit an exhaustive iterative multi-parametric search. In fact, the possible independent design parameters that must be studied even in the case of a 'simple' spur gear configuration comprise i.e. module, addendum, profile shift, tooth thickness, dedendum, cutter tip radius, pressure angle, face width etc, thus already numbering 8 parameters. The study is further complicated by the possibility to adjust each parameter for each gear separately. More crucially, it is important to consider the choice of these parameters in the early stage of the design, and in full consideration of the couplings (and constraints) that govern their feasible choices. The part of the design space that is not excluded because of aforementioned constraints can then be subject to parameter selection and possibly a design

* Corresponding author at: Faculty of Industrial Design Engineering, Delft University of Technology, Landbergstraat 15, 2628CE Delft, Netherlands.
E-mail addresses: c.spitas@tudelft.nl, cspitas@gmail.com (C. Spitas).

http://dx.doi.org/10.1016/j.mechmachtheory.2016.11.012
Received 18 August 2016; Received in revised form 20 November 2016; Accepted 21 November 2016
Available online 09 December 2016
0094-114X/

Nomenclature

Gear description & indices

α_0	pressure angle
a_{12}	nominal centre distance
α_c	operating pressure angle
α_0"	pressure angle at tip of tooth
b	tooth width
$c_c(c_{ci})$	cutter tip radius coefficient (of gear i)
$c_f(c_{fi})$	dedendum coefficient (of gear i)
$c_k(c_{ki})$	addendum coefficient (of gear i)
$c_s(c_{si})$	tooth thickness coefficient (of gear i)
$c_m(c_{mi})$	profile shift coefficient (of gear i)
$c_{sg}(c_{sgi})$	thickness coefficients at the base circles (of gear i)
r_s	form circle radius
$\acute{t}$	trochoid tip thickness of the generating rack tooth (sharp tooth)
m	module
$\overrightarrow{O_1R}$	vector from centre of gear i to intersection point
$\overrightarrow{A_1^{(n)}A_1^{(n+1)}}$	vector from two consecutive points on the tooth profile geometry of the gear number one
R	intersection point of tooth profiles
$\vec{t}_i(r_i)$	tooth flank vector equation of gear no. i
$i_{1,2}$	gear transmission ratio
O	centre of reference coordinate system
θ_i	angular position (of gear i)
$d\theta_i$	angular velocity (of gear i)
$r_b(r_{bi})$	base circle radius (of gear i)
$r_o(r_{oi})$	radius of pitch circle (of gear i)
$r_g(r_{gi})$	involute base radius (of gear i)
$r_k(r_{ki})$	outside radius
$r_f(r_{fi})$	inside radius (of gear i)
ε	contact ratio
t_b	base pitch (ref. to involute)
t_R	circular pitch
*	(as subscript) ref. to non-dimensional gear
i	ref. to gear no. i
x	addendum modification coefficient
N_i	number of teeth (of gear i)
A_i	point on profile of gear i
$\overrightarrow{O_iO_j}$	vector from the centre of gear i to the centre of gear j
$\overrightarrow{O_iK_j}$	vector from the centre of gear i to the tip point of gear j
O_i	centre of gear i
ξ_1	unitary vector of $\overrightarrow{A_1^{(n)}A_1^{(n+1)}}$
ξ_2	unitary vector of $\overrightarrow{O_1K_2}$
K_i	single ref. point at the corner of gear no. i
φ_{si}	angle corresponding to the tooth pitch thickness of gear i
ϑ	Poisson's ratio
ρ_i	radii of curvature at the point of contact of gear i

optimisation study. Already, in the automotive and aerospace industry every major company is developing and exploring its own class of non-standard designs and continuous improvements are being sought to achieve higher compactness, higher strength and load carrying capacity, improved dynamics with reduced noise and vibration signatures, in particular with regard to performance under partial or reversing loads, whining, rattling etc.

Several but limited studies and supporting models exist for this kind of design space exploration: Dedicated studies exist i.e. for the influence of module [7,13], addendum [14–22], profile modification [23–29] tooth thickness [30–36], dedendum [37–42], cutter tip radius [43–46], pressure angle [47–54], etc, but without considering the simultaneous manipulation of other design parameters as well, typically assigning standard values to the latter. Additionally, many researchers have investigated the influences of each design parameter for different applications such as contact analysis [55–63], stress [64–71], vibration [72–78], dynamics [79–88], cracking [89–93], lubrication [94–101], etc, but with similar limitations to their scope of the design space. Furthermore, the knowledge present in industrial publications/ technical reports is on the other hand very specific to given machine applications and not easily generalizable or verifiable.

Hereunder we provide some selective examples of the aforementioned limitations in scope, which, while justified or necessary in the context of the respective studies, mean that the possibility to generalise the results without additional modelling is likewise limited:

1.1.1. Dedicated parametric studies

- Module: E.g., with regard to the influence of the module, Nonaka et al [13] studied the strength of spur gear teeth with small modules of the order of 0.1 to 1.0 mm by using a specially designed gear test rig. The failure mode of gear teeth was observed for both tempered and soft nitrided gears. A sign of uneven contact along face width was found only for very small gears of modules 0.1 and 0.2 mm, which was very unlikely for such high precision in alignments of gear axes. Influences of the choice of pressure angle or tooth proportions were not considered, limiting the scope of the study.
- Addendum: With regard to the effect of addendum, e.g. Li [15] investigated its influence on the tooth surface contact strength and the bending strength of spur gears. Finite element analysis, the method of mathematical programming and teeth contact model were utilized to lead the contact analyses of the loaded teeth, calculation of stress and deformation of spur gears with not the same contact ratios and addendums. Load-sharing rate, root bending stress, contact stress, mesh stiffness and also the transmission error of the spur gears were analysed. It was detected that the number of contact teeth can be increased with increasing the amount of addendum, in addition, the contact & root bending stresses can be reduced with this kind of increasing. The effects of cutter tip radius (hence fillet radius), pressure angle etc parameters were not accounted for in this study.
- Profile modification: E.g. Lin et al [28] investigated the influence of parabolic and linear profile modification on low contact ratio of spur gears tooth with regard to the dynamic response. The influence of the modification zone's length and the whole

modification were calculated at different speeds and loads for obtaining the optimum amount of profile modification with regard to the minimum dynamic loading. A novel design charts were presented that have been included the non-dimension maximum dynamic load curves. The charts were applied at several loads using various profile modification. Minimisation of the dynamic loads can be defined from the charts taking ino the account the optimum amount of profile modification. Several design parameters having an influence on the tooth stiffness function, including pressure angle, addendum and root fillet were not in the scope of this study.

- Tooth thickness: E.g. Hsu and Su [30] proposed a novel approach by using a modified adjustable tooth thickness hob to decrease the tooth flank twisting of a crowning gear with the same centre distance. The topologies of the tooth surface, static transmission error and contact ellipses were also investigated in this work using adjustable tooth thickness of the modified hob. For demonstration and verification of the competence of the proposed gear hobbing method (considering the longitudinal crowning), there examples were studied. While the methodology proposed is readily generalizable, it is e.g. not clear how well the results would hold if different tooth proportions and corresponding contact ratios would be used.
- Cutter tip radius: E.g. Spitas et al [43] proposed non-dimensional multi-parametric analytical model to determine corner contact and penetration at the root of the gear tooth to find the influence of the design parameters (i.e. number of teeth, cutter tip radius, dedendum, addendum and contact ratio) on the possibility of the interference. Based on this approach, novel design guidelines for nonstandard compact tooth (short dedendum, large root fillet) were presented.

Spitas and Spitas [45] applied finite element method to investigate the bending strength for two kinds of fillet, the circular fillet and the trochoidal fillet. The results showed that for the number of these higher than seventeen, the bending strength of both fillets are equivalent circular fillet can be used instead of trochoidal fillet. However, in both aforementioned studies the results can be expected to vary significantly if larger values for the pressure angle were used.

- Pressure angle: E.g. Lin [53] presented an analytical model for meshing of planar gears considering the typical geometry of the gear tooth profile. The angular displacement of gears was presented as a function of pressure angle. Different pressure angle functions could produce different gear tooth geometries. Although the new methodology can be used for any kind of gear mesh, nevertheless the possible variation of other tooth geometrical characteristics, such as addendum, was not in the scope of this study.

1.1.2. Application-driven parametric studies

- Contact analysis: E.g. Medvedev et al [55] presented an analytical modelling for contact analysis of multi-pair gear. The parabolic function of transmission errors was applied for contact pressure. The precise transmitted torque and force of each contact pair and the contact pressure of the multi pair contact were determined by means of a new algorithm. The algorithm can be used for any kinds of gears and an example of spiral bevel gear has been applied for demonstration.
- Generation, contact and stress analysis: E.g. Litvin et al [70] represented computerised improvements in generation, design, stress analysis and simulation of gear meshing. A modified algorithm of tooth contact analysis and a new parabolic function of transmission errors designed for noise simulation. The proposed developments have been demonstrated for the design and simulation of three kinds of gear drives (spiral bevel gear, face-gear, modified helical gear). While the approach is very general, it does not readily afford the correlation of specific design parameters to behaviours without a dedicated study.
- Vibration: E.g. Farshidianfar and Saghafi [75] applied Melnikov analysis to investigate the chaotic performance of a gear system. The dynamic model of the gear system included the time varying mesh stiffness, backlash, static transmission error and external excitation. The initial values of the control parameter for the occurrence of divergence and chaos were predicted by the proposed analysis. Moreover, for verification of the analytical approach, the numerical bifurcation analysis and numerical simulation of the system were applied. As typical in such studies, the focus was not on parametric analysis that could produce direct design insights without further study.
- Dynamics: E.g. Faggioni et al [83] developed a Random-Simplex optimization algorithm to find the optimum amount of profile modifications for vibration redaction of a gear system using a nonlinear dynamic model. The good results were achieved by using high contact ratio gear properties and the proposed optimisation methodology. The scope of this study did not cover variations in the pressure angle.
- Cracking: With regard to tooth root cracking, e.g. Pandya and Parey [92] studied the influence of the gear design parameters (such as: root fillet radius, pressure angle, backup ratio) and the effect of the crack path on time varying gear mesh stiffness. A cumulative reduction index has been proposed for investigating the crack propagation in a tooth root using 2D finite element analysis. The percent change in the time-varying mesh stiffness has been determined by using variable crack intersection angle approach and a model of total potential energy. However, the influence of addendum (or whole depth) was not in the scope of this study.
- Lubrication: E.g. Larsson [100] analysed the transient non-Newtonian elastohydrodynamic lubrication of an involute spur gear. Taking into the account the influence of fluid transition, the film thickness of the lubricant and the pressure were calculated. In addition, considering the influence of shear strength restriction, it has been assumed that the model of the fluid was a non-Newtonian model and the film lubrication was isothermal. The results indicated that the influence of fluid transition was prominent at the transitions of the load. Once the load was increased (almost doubled), the minimum amount of film thickness was enlarged for a while because of the squeeze effect. At several points of contact, the stresses of subsurface and the factor of

friction were evaluated. In this study, two types of oil (poly-α-olefin & paraffinic mineral) were used as lubricant. Effects of pressure angle and addendum were not considered.

Although all above mentioned examples of studies contribute significantly to the knowledge base that is relevant to gear design, each of them (justifiably) deals with interrelated design parameters in the separate contexts of their own focal areas- particularly the module, pressure angle and addendum seem to always be treated as decoupled design choices and there is little information about synergies (or conflicts) in the choice of these parameters. As such, they do not offer a comprehensive model that can account for interactions between these parameters. I.e. changing the module and the pressure angle of one gear at the same time may have synergistic or conflicting effects, when meshing with another gear, possibly leading to improved strength or interference; pressure angle and addendum choices can result in strength improvement, but also undercutting; the cutter tip radius choice for one gear may cause interference with the addendum choice for the mating gear [43,44] etc. These types of couplings, which either affect *manufacturability (e.g. undercutting)* or *geometrical compatibility (e.g. interference)*, have not so far been addressed comprehensively in the literature in a coupled sense.

In the presence of such overwhelming complexity, the predominant answer has been standardisation of gear design parameters and combinations thereof [8–12]. Traditional gear design is generally based on standardised cutting tools, which makes the design of gears simple and available for any application. The drawback is that standard gear designs are known to have less than optimum performance in a range of applications, such as very high power density, high power-to-weight ratios, metal-to-plastic replacement, low-cost, compact, and low-vibration powertrains, which need to be designed with non-standard parameters. This becomes especially relevant as new production methods rely much less on standardised tooling, especially if non-generating processes are employed, i.e. broaching, injection moulding, sintering etc.

This paper aims to enable the multi-parametric design of gears in consideration of the major identified couplings between design parameters that limit or otherwise constrain the design space. Explicitly, the occurrence of undercutting and interference will be related to the combined values of the gear cutter pressure angle, module, number of teeth, cutter tip radius, dedendum, addendum, tooth thickness of each of two gears in a pair. The order of complexity is reduced my means of non-dimensionalisation with respect to the module, as well as the analytical coupling of some of these apparently independent parameters. The resulting model is both complete and computationally lightweight, to allow its use during the conceptual design and corresponding exploration of the design space.

As this work is focused on geometrical compatibility, the implications of parameter choices on stresses, load-carrying capacity, stiffness, dynamics etc are not considered herein. These will be the object of a subsequent study.

1.2. Manufacturability and geometrical compatibility as two considerations of gear design

1.2.1. Manufacturability (tip pointing, undercutting)

The first thing to be addressed in design is the matter of feasibility of a particular gear geometry choice: Can it be manufactured as intended? Except in the case of direct gear design [97–100], where gear geometry is directly and explicitly defined, typical design procedures define the gear geometry implicitly, based on basic gear rack parameters. In this sense, it can be that the gear produced by the manufacturing process deviates from the expected form due to the occurrence of secondary cutting action by the rack cutter, which manifests as either tip pointing or undercutting.

1. Tip pointing, which is essentially the elimination of the tooth top land and potentially the reduction of the tooth whole depth, can result from the use of a large pressure angle, and/ or addendum, or large positive profile shifting [2].
2. Undercutting is the condition where additional material is removed from the root of the tooth, potentially also removing part of the lower involute profile. It can result from the use of small numbers of teeth, small pressure angles, and/ or small cutter tip radii [2].

Tip pointing concerns the involute geometry exclusively and is as such very straightforward to calculate [1,36,102]. On the other hand, undercutting prediction concerns both the involute flank and the non-involute root segments and as such requires a more involved calculation. A number of analytical models for undercutting have been proposed, of which the more accurate ones include the effect of tip rounding, which introduces an additional parameter that in effect removes material from the cutter tip and lessens the propensity to undercut.

With regard to tip pointing in particular:

- Litvin [1] studied the occurrence of tooth tip pointing taking into the account that at the tooth top land and the two surfaces of the tooth will intersect. In order to solve this problem, a numerical program was presented. Different conditions were presented to avoid tooth pointing for modified involute gears, Novikov–Wildhaber helical gears and face-gear drives.
- Townsend [2] presented a calculation to determine the minimum tooth thickness that will produce tip pointing. Both long and short addendum scenarios were considered.
- Kapelevich [102] showed that tooth tip pointing in an asymmetric gear could be generated using positive profile shift for a number of teeth less than 17, resulting in the increase of load carrying capacity.
- Marita [6] investigated the effect of positive profile shift modification on tooth tip pointing. With increasing the positive shift, teeth became more pointed. This phenomenon was termed ‘Peaking’.

- Rackov et al [103] applied a generalised particle swarm optimisation algorithm for high contact ratio gears. It was found that with increasing the amount of addendum tip pointing could occur. To avoid this, all the constraints and equations were checked and the optimum amount of profile shift modification and addendum were calculated with the proposed optimisation methodology.
- Arikan [104] studied the determination of the addendum modification coefficient for spur gears operating at non-standard centre distances considering the avoidance of tooth tip pointing and undercutting. The performance a gear was optimised with regard to the addendum modification coefficient, taking into the account the amount of dedendum, centre distance, clearance, backlash, gear ratio, contact stresses and root stresses.
- Bair [105] investigated a three-dimensional geometric pointed tooth of an elliptical gear crowned along the major axis. The gear drive was designed to avoid edge contact while there was an axial misalignment. The rack cutter was used for developing an analytical model of the gear drive. Moreover, a numerical program was computed for generation gear tooth without pointed teeth.

In the traditional theory of involute meshing, there is a minimum number of teeth to avoid undercutting of the root by the generating rack/ tool, i.e. for many 20-degree involute pinions this minimum number is 17. However, such rules of thumb are of little use when dealing with non-standard designs, in which case more detailed models are appropriate:

- Litvin [1] defined the limit condition for tooth undercutting that the tooth has been generated by means of rack-cutter taking into the account the meshing between involute part of the gear and the straight line of the rack cutter.
- Townsend [2] and Spotts [4] showed that for each pressure angle there is critical number of teeth that undercutting happens when the addendum coefficient equals 1.0 and the profile shift coefficient is zero. I.e. for spur gears with pressure angles of 14½°, 20° and 25° the tooth root undercut occurs with a number of teeth lower than 32, 17 and 12, respectively.
- The undercutting conditions for symmetric spur gears which have been designed directly are not subject to the restrictions of the generating rack and its profile shift coefficient [36,102].
- Alipiev et al [106] proposed a generalised approach to describe tooth undercutting. In this study, three kinds of conditions were defined for undercutting of spur gear tooth. The first one which was the traditional undercutting boundary condition called “undercutting-type I”. The second and the third were described as “undercutting-type II_a” and “undercutting-type II_b”. Based on this study, type II_a and type II_b undercuts were made by the tip rounding of the rack cutter, whereas the type I was made by the straight line of the rack cutter profile. Moreover, the conditions for preventing undercutting of all the three typed were presented considering the amount of fillet radius of the rack cutter
- He et al [107] presented a theoretical study and numerical simulation for undercutting occurrence. Minimum number of the involute gear teeth without undercutting was found in two different approaches as the traditional boundary condition and cutter tip radius limitation. The results indicated that the minimum number of teeth without undercutting considering traditional restriction is less than the cutter tip radius limitation.
- Brauer [108] presented the analytical relations for a straight conical involute gear tooth surface and its offset surface to avoid undercutting occurrence. In this study, Merritt’s [5] formulation for undercutting restriction was applied for the modelling. A developed expression for undercutting check was presented considering the amount of addendum modification.
- While the starting point of each of these models is the same, namely the geometrical simulation of gear-to-rack contact, the mathematical formulations present discrepancies in their predictions, as will be seen in Section 3.2.

Based on these models for the different undercutting conditions we calculate the minimum number of teeth to prevent undercutting as shown in Table 1.

In this work we perform an independent investigation of the conditions that lead to tip pointing and undercutting, in the course of which we explain also the discrepancies observed between the existing models.

1.2.2. Geometrical compatibility (interference)

Even if a gear is manufacturable, as per Section 1.1.1, it is not guaranteed that two gears configured in a pair and made to mesh will do so without geometrical interference. For this reason, there are guidelines in the standards, which steer parameter selection to subspaces in the design space where it is known a-priori that interference does not occur [101,102,106–111]. However, interference

Table 1
Comparison of undercutting equations for minimum number of teeth.

Researcher(s)	Minimum number of teeth to avoid undercutting
Litvin [1], Kapelevich [102], Alipiev (type I) [106]	$N \geq \frac{2(c_k - c_m)}{\sin^2 \alpha_0}$
Townsend [2], Spotts [4]	$N \geq \frac{2c_k}{\sin^2 \alpha_0}$
He [107]	$N \geq \frac{2(c_k + c_c)}{\sin^2 \alpha_0}$
Alipiev (type II) [106]	$N \geq \frac{c_c}{\sin \alpha_0}$
Merritt [5], Brauer [108]	$N \geq \frac{2(c_k - c_m - c_c(1 - \sin \alpha_0))}{\sin^2 \alpha_0}$

becomes a concern when non-standard tooth forms with reduced radial clearance are employed, such as large-fillet short-dedendum gears [38]. These tooth forms have shorter involute working flanks and excess material at the root, which can lead to non-conjugate corner contact and penetration at the tooth root. Existing models for interference are unable to predict this, or rely on calculation-intensive simulations, which make them impractical for design.

As with undercutting, simple analytical models exist and are widely used to predict interference [1,3]. However, these models have been proven recently to underestimate interference risk, and corner contact and penetration in particular, when small numbers of teeth are concerned, especially if compact low-dedendum gears produced with large cutter tip radii are concerned [38,39]. Interference for non-standard gears happens because of the penetration of the tip of the gear number 2 at the tooth root of the gear number 1. The new interference model has to cover the area of penetrating that occurs at the corner-to-root contact region. Furthermore, interference due to module/pressure angle compatibility, tooth width compatibility (backlash), and radial clearance compatibility are non-trivial factors that must be considered in non-standard gear design [112]. Thus in the case of non-standard and compact gear geometry, these new computational models have to be implemented in the context of multi-parametric design.

Based on these considerations, interference modelling can be categorised in four parts as:

1. Pitch compatibility: Normally the use of the same module and pressure angle for both gears in a mating pair, as dictated by all standards, is sufficient to guarantee pitch compatibility. In general, however, these may be assigned different values for each gear, as long as base pitch compatibility is maintained [112].
2. Thickness-wise interference: Negative backlash, i.e. due to errors in tooth thickness or centre distance, also leads to interference. It can be detected by observing only the conjugate parts of the profiles. Nonetheless, if the leading profiles are positioned in a compatible meshing position, seizure will manifest as corner penetration at the coast sides [49,112].
3. Radial interference: The concern here is that the radial clearance can be so small that the top land of one gear will contact the root of the mating gear [112].
4. Corner contact and penetration: While standards provide sufficient clearances to avoid interference for any selectable combination of the gear design parameters, this may not be the case in many non-standard and compact gear design configurations [38]. In those cases, it is possible that the corner of the tip of one gear tooth will contact and tend to penetrate the root of the mating gear tooth, causing interference.

Pitch compatibility, often taken for granted with standard mating gear pairs, is no longer guaranteed if module and pressure angle are free to vary between the gears. This is given special consideration in the present study, together with basic models for thickness-wise (backlash) and radial interference.

Furthermore, the well-known analytical solution which has been suggested by Litvin [1] is valid for studying interference occurring along the line of action only, which is a false premise in most non-standard and compact gear design configurations [38], where corner contact and penetration is a concern. In particular, the necessary and sufficient condition for non-interference at the root of the reference gear (gear 1) proposed by Litvin [1] and elaborated by the authors as follows [43]:

$$c_c \le c_f \tan\left(\frac{\pi}{4}+\frac{\alpha_o}{2}\right)\sec\alpha_o - \left(\sqrt{\left(\frac{1}{2}N_2+c_{k2}\right)^2-\frac{1}{4}N_2^2\pi^2\cos^2\alpha_o}-\frac{1}{2}N_2\pi\sin\alpha_o\right)\tan\left(\frac{\pi}{4}+\frac{\alpha_o}{2}\right)\tan\alpha_o \tag{1}$$

In fact, Eq. (1) only predicts a tangent to the exact interference limit curve and is generally not valid, except at sufficiently high values of c_c and c_f of gear 1 (Fig. 4). In this paper Eq. (1) still provides a useful limit-tangent to the exact interference limit curves, which are calculated by the corner contact-and-penetration model [43]. In this work we perform a synthesis of appropriate models for the four different types of interference, providing a comprehensive set of accurate multi-parametric mathematical conditions for the geometrical compatibility of gear pairs.

1.3. Standards and computational resources for implicit and explicit/ direct gear design

For the design of gear geometry, a number of established design solutions have been codified in standards for implicit gear design such as GOST 13,755 [113], ISO 53[114], NF E 23-011[115], ISO TR 4467 [116], JIS B 1702 [117], DIN 867 [118], AGMA 201.02 [119], DIN 3972 [120]. These standards have been implemented in dedicated gear design software such as KISSSoft [8], HyGEARS [9], Gear Design Pro [10].

Applicable standards also exist for explicit/ direct gear design, i.e. ANSI/AGMA1006-A97 [121], as well as dedicated books [102] and software, i.e. Gear Tooth Root Fillet Optimization Software [122].

Given that the above sources are fundamentally implementations of the models discussed under Section 1.1, they are also subject to the same critical considerations.

Where applicable throughout the paper, a few selected standard solutions and de facto industry solutions (‘best practices’) are shown in context in the enlarged design space, allowing a quick assessment as to how close they are to naturally emerging design limits (which are often associated with local optima).

1.4. Current study

In this paper, we start by introducing a non-dimensionalisation methodology (Section 2) to produce an elegant generalised

representation and reduce the order of the multi-parametric problem (Sections 5.1–5.3). The basic principles are introduced to frame a comprehensive manufacturability (tip pointing, undercutting) and geometrical compatibility (interference) model for the parametric design of profile-generated involute gears (Sections 3.1–3.4 and 4.1–4.5 respectively). The synthesised model simultaneously considers all applicable geometric and kinematical conditions and constraints to qualify each point in the design space (hence each combination of geometrical gear design parameters) in terms of manufacturability and geometrical compatibility.

The design parameters considered include the module, pressure angle, tooth thickness, addendum, dedendum, cutter tip radius, and number of teeth of each gear. While in principle the module and pressure angle may be varied between gears subject to specific constraints on pitch compatibility [113], in this study for simplicity the convention of choosing a common module and pressure angle for both gears in a mating pair is maintained. This reduces the considered design parameters from 14 to 12, all of which are in principle independent in the context of non-standard design. An extensive multi-parametric study is conducted over Sections 6.1.1–6.1.6, discussing the most notable effects of different choices for the considered design parameters.

To demonstrate the capabilities of the model, this paper proposes two geometric metrics that function as indirect performance indicators, which are relevant to gear design: a) Compactness (associated with strength and stiffness) and b) Contact ratio (associated with dynamics and peak-to-peak dynamical transmission error). These are discussed in Section 6.2. However useful, the proposed metrics are by no means exhaustive – they serve only to demonstrate the utility and additional insights obtainable by the developed multi-parametric model. For each performance indicator, given the multi-parametric nature of the problem, it is possible to dictate a-priori or restrict the range of certain parameters, thus limiting the search area for design space exploration (and the number of associated strength or dynamical simulations), or even suggest a global optimum at the boundary of the constrained design space.

Finally, design guidelines are extracted and multi-dimensional maps of the design space are given in terms of the aforementioned design parameters. Benchmarks against standards as well as known non-standard 'best industry practices' reveal significant potential in the less explored parts of the design space, especially with regard to a multitude of low-clearance, compact gear designs.

2. Non-dimensional modelling of spur gears

A non-dimensionalisation scheme is applied, which permits the simultaneous modelling of entire families of gears and lends wider generality to the results of the numerical solutions of this study.

As in previous studies [38–40,43–45,49,54,60,77,79,109,110,112,123], all geometrical features are non-dimensionalised in terms of the module. Hence any given feature f can be related to its non-dimensional correspondent f* by the formula:

$$f = mf^* \tag{2}$$

This is consistent with the stat-of-the-art use of non-dimensional coefficients, such as for addendum, dedendum, etc.

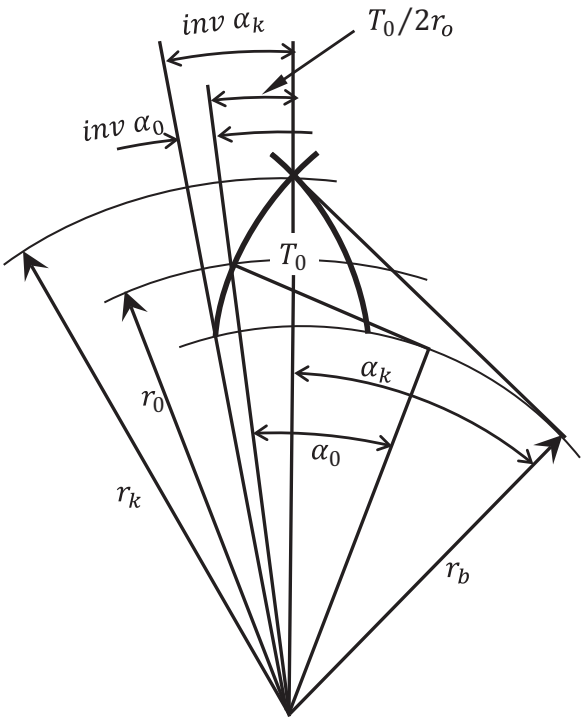

Fig. 1. Pointed tooth model as per Buckingham [3].

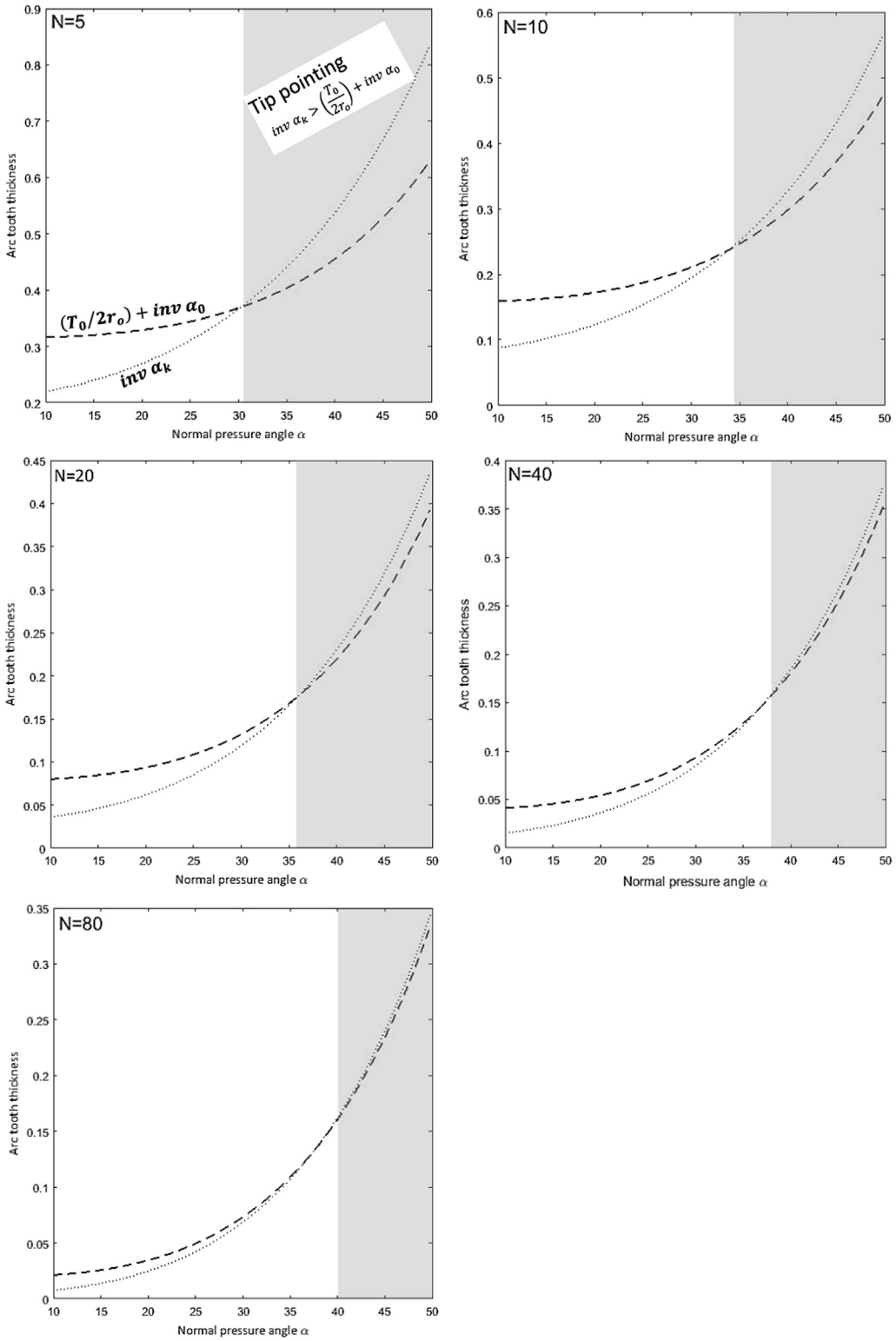

Fig. 2. Illustration of tip pointing area design according to the condition of Eq. (11) (c_k=1, c_s=0.5).

3. Manufacturability modelling

3.1. Tip pointing

Tip pointing is the condition where the top land of the teeth disappears, leaving both sides of the working tooth profiles (drive and coast) to intersect.

The shape of the tooth becomes more peaked or pointed and the tooth flank becomes more curved as the pressure angle increases (Fig. 1). Therefore, the top land becomes smaller and eventually results in pointed or peaked tip. Gear standards [113–121] recommended that the tip thickness should be greater than equal to 0.2 times the module for the hardened gears and this may be increased to 0.25 m in exceptional cases. The limitation of peaked or pointed tooth makes a boundary to the maximum amount of pressure angle. In turn, the maximum achievable outside diameters of such gears are a function of tooth thickness. For any given number of teeth, the tooth thickness can be increased such that the tip will become pointed at the outside diameter [2]. However, the resulting teeth do not have the correct whole depth because the involute curves cross over below the expected outside diameter (this phenomenon is termed 'peaking' [6]). The amount that the outside diameter of a gear is to be modified is usually a function of the tooth thickness desired.

The maximum amount that the tooth thickness of a gear can be increased to just achieve a pointed tooth can be found already in Dudley's Gear Handbook [2], reproduced here using an adapted notation:

$$c_k^{max} = \frac{N\left(inv\left(\cos^{-1}\frac{r_b}{r_k}\right) - inv\alpha_0\right) - \frac{\pi}{2}}{2\tan\alpha_0} \tag{3}$$

Where c_k^{max} is the maximum addendum coefficient at which a tooth having full working depth will come to a point,α_0 is standard pressure angle of the rack cutter and $\cos^{-1}\frac{r_b}{r_k}$ is pressure angle at tooth tip. To avoid pointed teeth and undercut root, it is needed to shorten the amount of addendum and working depth, however Eq. (3) cannot give us the condition of the avoidance of pointed tooth.

Buckingham [3] introduced a condition to avoid pointed tooth that the arc tooth thickness at outside radius (r_k) will be less than zero. With this regard, Fig. 1 is presented to formulate this condition [3].

Referring to Fig. 1, T_0 is the tooth thickness at the pitch radius (r_0),$inv\alpha_k$ and $inv\alpha_0$ are the involute function of α_k (pressure angle at r_k) and α_0 (pressure angle at r_0), respectively.

From Fig. 1, it can be obvious that:

$$\cos\alpha_0 = \frac{r_b}{r_o} \tag{4}$$

$$\cos\alpha_k = \frac{r_b}{r_k} \tag{5}$$

And

$$r_b = r_o\cos\alpha_0 \tag{6}$$

$$r_k = r_o + mc_k \tag{7}$$

From Eqs. (4) and (5), we have:

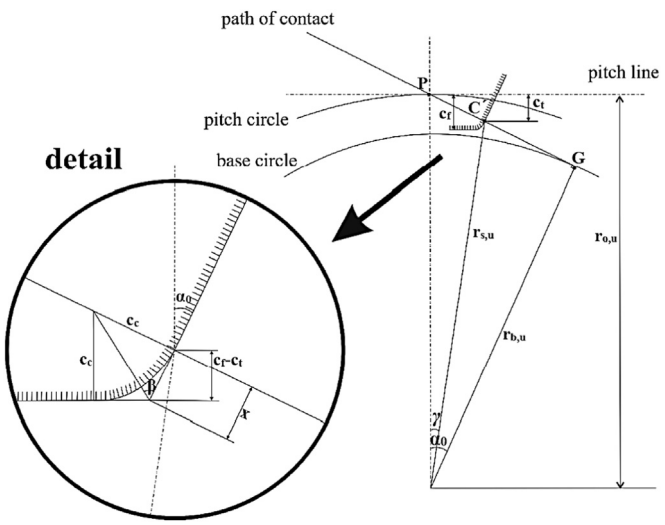

Fig. 3. Geometry of gear cutting at the tooth fillet [44].

$$\frac{r_b}{r_k} = \frac{\frac{N}{2}m\cos\alpha_0}{\frac{N}{2}m + mc_k} \tag{8}$$

The arc tooth thickness at the outside radius (r_k) can be presented as:

$$inv\alpha_k = (T_0/2r_o) + inv\alpha_0 \tag{9}$$

Which can be rewritten as:

$$inv\alpha_k = \left(\frac{\pi c_s}{N}\right) + inv\alpha_0 \tag{10}$$

With substituting Eq. (8) into Eq. (5) and then Eq. (10), the condition of avoiding tooth pointing can be presented as:

$$inv\left(\cos^{-1}\left(\frac{\frac{N}{2}\cos\alpha_0}{\frac{N}{2} + c_k}\right)\right) < \left(\frac{\pi c_s}{N}\right) + inv\alpha_0 \tag{11}$$

Illustration of Eq. (11) is presented in Fig. 2. The grey area corresponds to tooth pointing, which is undesirable for gear design.

3.2. Undercutting

Conditions of non-undercutting by a rack-cutter may be determined by using the general approach presented based on simple geometric considerations has been introduced by Litvin [1]. The geometry of gear cutting at the tooth fillet (gear not shown, only rack cutter tooth shown for clarity) has been further elaborated by the authors [44] and is shown in Fig. 2. According to this model the condition for non-undercutting is as follows:

$$\alpha_0 - \gamma \geq 0 \tag{12}$$

It follows from Fig. 3 that:

$$\gamma = \tan^{-1}\frac{\frac{c_t}{\tan\alpha_0}}{(r_{o,u} - c_t)} \tag{13}$$

Further substituting some details of Fig. 2 in Eq. (13) yields:

$$\alpha_0 - \tan^{-1}\frac{c_f\tan(45°+\frac{\alpha_0}{2}) - c_c\cos\alpha_0}{\tan\alpha_0[(r_{o,u} - c_f)\tan(45°+\frac{\alpha_0}{2}) + c_c\cos\alpha_0]} \geq 0 \tag{14}$$

According to research by He et al [107], if the rack addendum extends inside the point of tangency of base circle and pressure line (Point C' in Fig. 3), gear undercutting consequentially occurs. Therefore, the addendum of the rack must be under the theoretical contact point. The cutter centerline is tangent with the gears' reference circle. The requirement without undercutting for standard involute spur gears as follows:

$$GP\sin\alpha_0 \geq c_t \tag{15}$$

By substituting some details of Fig. 3 in Eq. (15) we obtain:

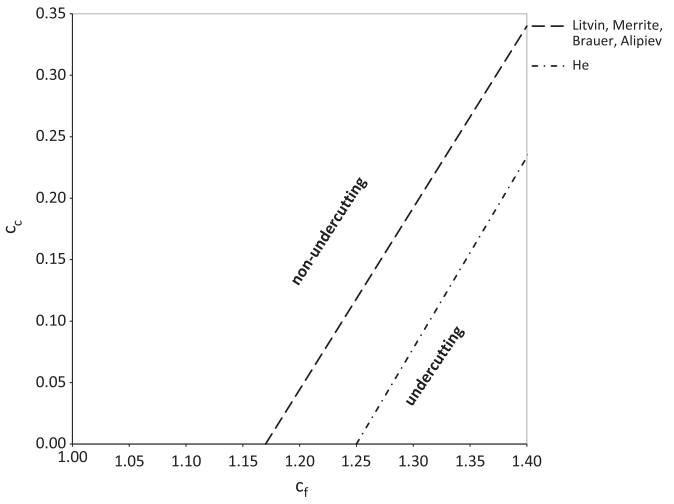

Fig. 4. Comparison of undercutting phenomena for different theories.

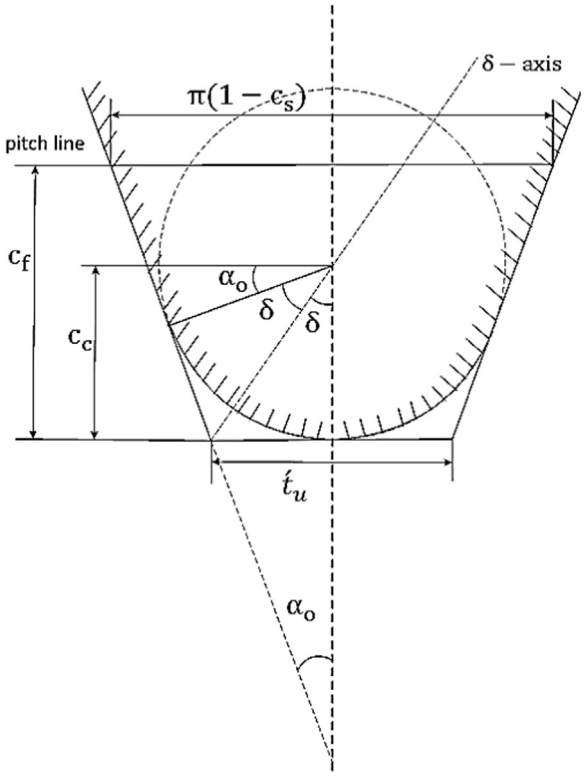

Fig. 5. Calculation of the tooth thickness for a given dedendum.

$$(r_{o,u}\sin^2\alpha_0 - c_f)\tan\left(45°+\frac{\alpha_0}{2}\right) + c_c\cos\alpha_0 \geq 0 \tag{16}$$

On the other hand, according to Merritt [5], Brauer [108] and Alipiev et al [106] (undercutting of type I) undercutting occurs (approximately) if the path of contact extends past the interference point. Therefore, a transverse plane of the tooth is not undercut if:

$$GP \geq C'P \tag{17}$$

And with same details of Fig. 3 in Eq. (17), leading again to Eq. (16).

The predictions from the three undercutting models derived in Eqs. (14), (16), (17) above are plotted and compared in Fig. 4. According to Fig. 4 the undercutting condition that has been introduced by Litvin [1], Merritt [5], Brauer [108] and Alipiev et al [106] has same results for undercutting and non-undercutting parts of spur gears.

It is apparent that Litvin's condition, as per Eq. (12), and Merritt's condition, as per Eq. (17), produce identical predictions for interference, which are more conservative than the predictions based on He's condition (Eq. (15)), where the combined influence of the dedendum coefficient and the rack cutter tip radius coefficient has been considered.

3.3. Tooth thickness analysis

Fig. 5 describes the case of maximum cutter tip radius $\max c_c$[43–45,123], where it can be observed that the tip thickness $\acute{t}_u$ of a sharp tooth of the non-dimensional rack cutter relates to the pitch thickness $\pi(1-c_s)$, the dedendum and the pressure angle according to the formula:

$$\acute{t}_u = \pi(1-c_s) - 2c_f\tan\alpha_0 \tag{18}$$

$$\max c_c\tan\delta = \frac{1}{2}\acute{t}_u \tag{19}$$

$$\max c_c = \frac{\acute{t}_u}{2\tan\delta} \tag{20}$$

Where, due to the symmetry of the fillet around the δ-axis:

$$\delta = \frac{1}{4}\pi - \frac{1}{2}\alpha_0 \tag{21}$$

To calculate the tangent of δ we apply on Eq. (21) a trigonometric identity, which yields the expression:

$$\tan\delta = \sec\alpha_0 - \tan\alpha_0 \tag{22}$$

Therefore by combining Eqs. (18), (19), (20) and (22) we obtain:

$$\max c_c = \left[\frac{1}{2}\pi(1-c_s) - c_f\tan\alpha_0\right](\sec\alpha_0 - \tan\alpha_0)^{-1} \tag{23}$$

Notice that application of a larger radius than that calculated from Eq. (23) would result in an undercut cutter tooth, having a smaller whole depth and c_f value than intended.

3.4. Form radius analysis

By exploiting the symmetry of the rack cutter tooth as shown in Fig. 3 the following relationship is deduced:

$$\beta = \frac{\pi}{4} + \frac{\alpha_0}{2} \tag{24}$$

Also:

$$\tan\beta = \frac{c_c}{x}c_f - c_t = x\cos\alpha_0 \tag{25}$$

And therefore:

$$c_f - c_t = c_c\frac{\cos\alpha_0}{\tan(\frac{\pi}{4} + \frac{\alpha_0}{2})} \tag{26}$$

Having defined point C' as the intersection of the line of action GP and the ξ-axis offset by c_t, it is possible to calculate the form radius as:

$$r_{s,u} = \sqrt{\left(\frac{c_t}{\tan\alpha_0}\right)^2 + (r_{o,u} - c_t)^2} \tag{27}$$

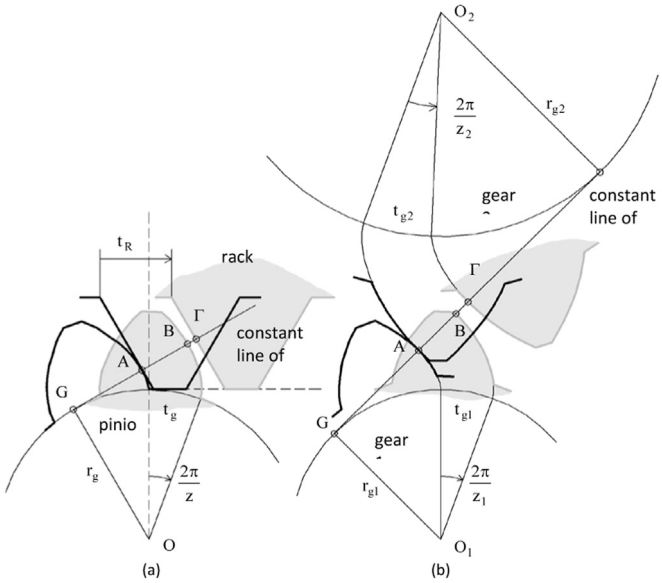

Fig. 6. Pitch compatibility: (a) pinion-rack, (b) pinion-wheel [54,112].

4. Geometrical compatibility (interference) modelling

4.1. Pitch compatibility

In this study, we use the conditions for pitch compatibility developed by Spitas [54,112]. In Fig. 6 terms of r_{g1}, r_{g2}, N_1, N_2 are base radius of gear 1, base radius of gear 2, number of teeth of gear 1 and number of teeth of gear 2, respectively.

From the properties of the involute, we can have:

$$AB = t_{g1}, \quad A\Gamma = t_{g2} \tag{28}$$

Therefore for pitch compatibility the necessary condition ca be defined as:

$$t_{g1} = t_{g2} \tag{29}$$

By applying the properties of the involute curve:

$$AB = t_g \tag{30}$$

From Fig. 6, It can be proved that:

$$A\Gamma = t_R \cos\alpha_0 \tag{31}$$

Then the necessary condition for pitch compatibility can be written as:

$$t_g = t_R \cos\alpha_0 \tag{32}$$

The following conclusion can be derive from Eq. (32):

Gears of the same base pitch t_g can be generated by two different racks defined by t_R, α_0 and t_R', α_0', if and only if:

$$t_R \cos\alpha_0 = t_R' \cos\alpha_0' \tag{33}$$

4.2. Thickness-wise interference: Seizure

The pair of involute gears illustrated in Fig. 5. The general condition for sufficient tooth backlash is derived [54]:

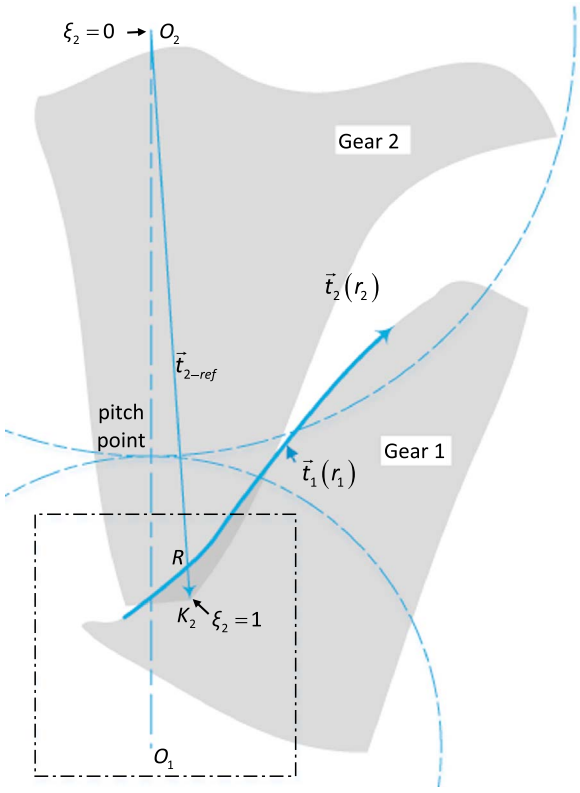

Fig. 7. Corner contact and penetration model [43].

$$(\alpha_c - \tan\alpha_c)\frac{N_1 + N_2}{\pi} \leq 1 - c_{sg1} - c_{sg2} \tag{34}$$

Where α_c is the operating pressure angle, c_{sg1} and c_{sg2} are the coefficients of tooth thickness at the base circles for gear 1 and 2, respectively.

4.3. Radial interference

One of the main constraints for fillet optimisation is a minimum radial clearance. Radial clearance results from the difference between addendum and dedendum of two mating gears, with standard radial clearance coefficients varying from 0.2 to 0.35. For avoidance of the tooth tip/root interference, the minimum amount of clearances must be greater than zero. This may necessitate the

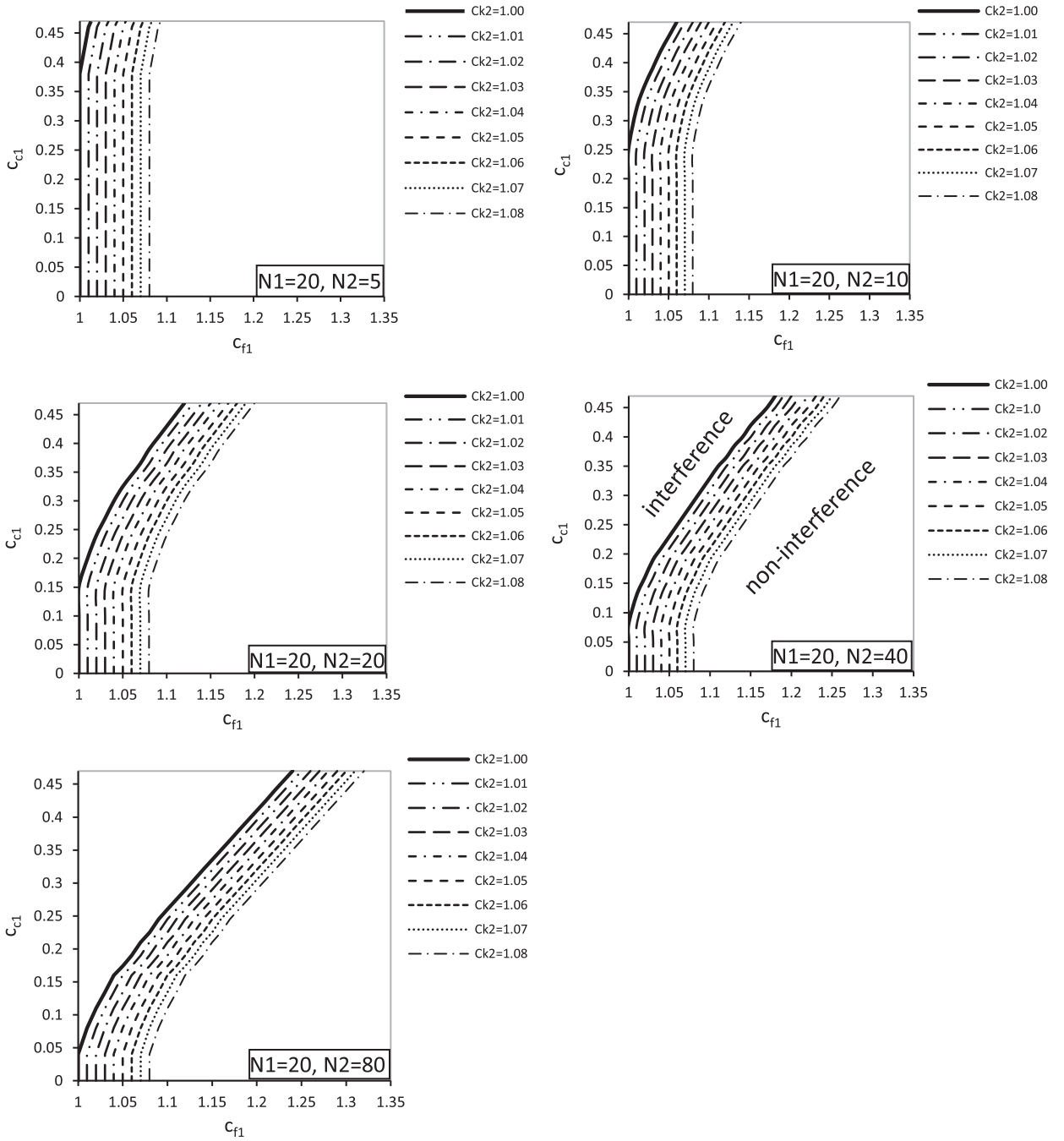

Fig. 8. Detection of interference and non-interference are for different combination of the design parameters including addendum coefficient of gear 2 (c_{k2}).

tooth root with increased clearances even with some reduction of tooth bending stress [54,124]. There should be a minimum amount of allowable radial clearance that the conjugate gears can operate without the risk of seizure. The following relationships must be true for assuring radial clearance:

$$r_{k1} + r_{f2} \leq a_{12} \tag{35}$$

$$r_{k2} + r_{f1} \leq a_{12} \tag{36}$$

That r_{f1} and $r_{f2}$are the inside radii of gear 1, 2, r_{k1} and r_{k2} are the outside radii of gear 1, 2, and a_{12} is the centre distance of the gear pair.

Furthermore, Eq. (36) can be reworked into the following form, considering that nominally $a_{12} = r_{o1} + r_{o2}$

$$c_{f1} - c_{k2} + 1 \geq 1 \tag{48}$$

and introducing the notation:

$$c_{f1eqv} = c_{f1} - c_{k2} + 1 \tag{46}$$

Eq. (48) takes the form:

$$c_{f1eqv} \geq 1 \tag{49}$$

A similar condition can be formulated from Eq. (35) for gear 2. The significance of c_{f1eqv} will be revisited in Section 4.5.

4.4. Corner contact and penetration

A detailed study of interference resulting from corner contact and penetration can be found in Spitas [43] (Fig. 7). Here we summarise the main considerations and adapt the model to the present study.

Consider two parametric curves $\vec{t}_1(r_1)$, $\vec{t}_2(r_2)$ defining correspondingly two mating tooth flanks. During a mesh cycle, these flanks will engage in conjugate action around the pitch point, and will each rotate according to a known law of the form:

$$i_{12} d\theta_2 - d\theta_1 = 0 \tag{37}$$

For two meshing gears at the pitch point, the following condition must be true:

$$\theta_2 = \theta_1 = 0 \tag{38}$$

Considering Eq. (37), Eq. (38) in the case of constant transmission ratio integrates over time for the leading side to:

$$i_{12}\theta_2 - \theta_1 = 0 \tag{39}$$

And for the coast side to:

$$i_{12}(\theta_2 - \varphi_{s2}) - (\theta_1 - \varphi_{s1}) = 0 \tag{40}$$

Where φ_s is:

$$\varphi_s = c_s \frac{2\pi}{N} \tag{41}$$

That φ_s represents the angle to the tooth pitch thickness of each gear.

The tip of each tooth may (or not) penetrate the other near the vicinity of its root which depends on each tooth shape. Such corner penetration is shown in Fig. 7. The location of the corner point K_2 is easily found as:

$$\vec{t}_{2-ref} = \vec{t}_2(r_{2-ref}) \tag{42}$$

Considering the vector descriptions for the curvet_2 and the line O_2K_2, in mathematical terms this translates to the requirement that two real numbers r_1 and ξ_2 exist such that the following conditions are simultaneously true:

$$\overrightarrow{OO_1} + \vec{t}_1(r_1) = \overrightarrow{OO_2} + \xi_2 \overrightarrow{O_2K_2} \vec{t}_1(r_1) = \overrightarrow{O_1O_2} + \xi_2 \vec{t}_2(r_{2-ref}) \tag{43}$$

$$r_1 \in T_1 \tag{44}$$

$$0 \leq \xi_2 \leq 1 \tag{45}$$

Where O is the centre of any arbitrary reference coordinate system.

Equivalent discreet models suitable for working with numerical point cloud representations of the tooth surfaces can be found in Spitas [43]. The can be used alternatively to Eqs. (43)–(45).

4.5. Addendum and dedendum analysis

By means of the corner contact and penetration method from Section 4.4, interference and non-interference design space for different combinations of the design parameters are presented in Fig. 8. The design parameters are included as the number of teeth

for gear 1 and 2, cutter tip radius coefficient of gear 1, dedendum coefficient of gear 1 and addendum coefficient of gear 2.

According to the results of Fig. 8, there is a relation between dedendum coefficient of gear 1 (c_{f1}) and addendum coefficient of gear 2 (c_{k2}).

The relation is introduced as follows, same as in Eq. (46):

$$c_{f1eqv} = c_{f1} - c_{k2}+1$$

Introducing this equivalent metric for c_f, which notably takes into account the mating gear as well, each family of curves is reduced to a single curve (coincident with each thick black line in Fig. 8).

5. Parametric couplings and synthesis of generalised model

5.1. Parametric couplings

We notice the following important couplings between gear design parameters:

- Normally, it is considered that the pressure angle of two mating involute gears has to be the same, in order to allow them to mesh. However, it follows from basic geometry that any involute will fulfil the necessary tangency conditions when mating with any other involute, so the actual concern is pitch compatibility: base pitch compatibility in particular. In fact, gears with different pressure angles may still mesh properly if they have the same base pitch, which can be obtained by a proper selection of the individual (non-standard) gear modules. In this sense, base pitch compatibility imposes a strong coupling between the pressure angle and module.
- Although in principle the addenda and dedenda of a pair of gears (4 parameters in total) may be selected arbitrarily, the predicted interference behaviour can be expected to depend on two distinct combinations involving the addendum of one gear and the dedendum of the other gear, as demonstrated in Section 4.4. Clearly, increasing the amount of addendum of one gear will necessitate and increase in the dedendum of the mating gear.
- Tooth thickness and pressure angle are related with regard to tip pointing. With increasing the pressure angle it will be necessary to increase tooth width in order to avoid tip pointing. Addendum and dedendum (hence whole depth) are likewise coupled with tooth thickness and pressure angle in the same context, with shorter teeth being less prone to tip pointing even for large pressure angles and small tooth widths. This is shown in Section 3.1.
- Dedendum, cutter tip radius and pressure angle can be expected to have a combined effect on the occurrence of undercutting, as shown in Section 3.2.
- Thickness-wise interference between two gears can be expected to depend on tooth thickness, the operating pressure angle, and the numbers of teeth of both gears, all coupled as shown in Section 4.2.
- Considering radial interference at the root of one gear mating with another gear, it has been shown in Section 4.3 to depend on the relation between dedendum of the reference gear, the addendum of the mating gear, and the numbers of teeth of both gears. The same consideration is valid for radial interference at the root of the mating gear.
- Addendum, cutter tip radius, pressure angle and tooth thickness are in principle properties of the rack cutter (and cutting layout). As shown in Section 3.3, not every combination is viable: i.e. a large cutter tip radius must be accommodated by correspondingly large thickness and/ or large pressure angle and/ or small addendum. While each one of these 4 parameters is in principle independent, the limits on each one are strongly coupled.

Thus hereinafter we shall consider the above couplings and the corresponding developed models to describe and support the relevant design choices.

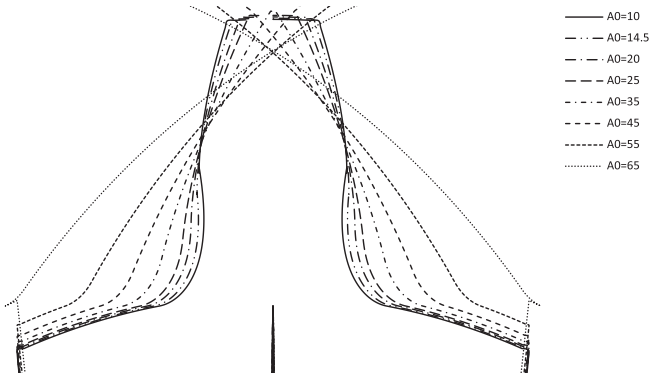

Fig. 9. Tooth profile geometry with different pressure angle.

5.2. Design parameters

Hereunder some of the considered parameters are discussed, summarising the main considerations typically at play in the context of gear design. This section, together with Section 5.1, serves to support the condensed synthetic overview produced in Section 5.3.

5.2.1. Pressure angle (α_0)

Pressure angle is the slope of the gear tooth at the pitch point. If the pressure angle were 0°, the tooth is parallel to the axis of the gear- and is really a spur-gear tooth. Generally, gears can be manufactured with different type of pressure angles of 14.5°, 20° and 25° in industrial applications.

Increasing the bending strength can be done by applying high pressure angles bigger than 22.5, although the gear engineers are in favour of 20° pressure angle gears [2]. To obtain the higher contact ratios, gears with low pressure angles (smaller than 15°) were in used, nevertheless low pressure angle are not common because of undercutting tooth root and lack the load-carrying capacity.

Gears generated with non-standard pressure angle have been demonstrated to achieve higher bending strength [54]. In fact, the same working flank can be cut by infinite combinations of pressure angles and modules [47–54], but with varying implication on the produced root shape and strength. Practical limitations to using high pressure angle values arise from unwanted tooth tipping (Fig. 9) and corresponding addendum reduction, as well as increased radial force and bearing load components.

Fig. 9 shows the geometry of on tooth of a spur gear with different pressure angle. With different value of the pressure angle, a different part of the same involute will be produced (e.g. if applying profile shift), or possibly an entirely new involute. Increasing the pressure angle tends to increase the tooth root thickness, strength and consequently the load carrying capacity.

5.2.2. Module (m)

Geometrically speaking the module is just a scale factor for a gear. For instance, all geometrical features of a spur gear with m=2 *mm* are two times bigger than the corresponding features of a m=1 *mm* gear, provided that the number of teeth, nominal pressure angle and the whole depth, fillet radius, backlash and profile shifting coefficients are the same. All linearly affected magnitudes (i.e. root stress including stress concentration, sliding velocity etc.) increase either proportional (sliding velocity) or inversely proportional to it (root stress), while others (i.e. contact stress) follow a non-linear relationship. Regarding the efficiency of a gear pair it is mainly dominated by the sliding velocities of the gears in mesh along their path of contact, therefore the bigger the module the higher the losses for a given angular velocity and transmission ratio.

5.2.3. Cutter tip radius (c_c)

The root fillet of a tooth in normally generated by the cutter tip trajectory. The root carries the maximum bending stress of the tooth, and therefore the value of the cutter tip radius has a significant effect on tooth bending strength. Increasing the cutter tip radius results in larger generated root fillet therefore reducing stress concentration and the value of the maximum root stress.

At the same time, a larger cutter tip radius tends to reduce the involute part of the tooth, thereby increasing the risk of interference with mating gears and limiting the values that may be applied practically.

Other considerations are:

- Small or zero radius has been known to cause localised tool wear, causing in turn poor surface quality and dimensional inaccuracy of the manufactured gear
- For a given whole depth, there is a practical limitation on the maximum radius that is obtainable; the larger radii will be incompatible with the designated whole depth for the 20° gear system, or the cutter teeth will be undercut, i.e. they cannot be realised unless the whole depth is reduced

.

Table 2
Dependency of the design parameters.

Design parameters (one per gear)	Dependency	Explanation
α_0	$\alpha_{01} = \alpha_{02}=\alpha_0$ or same base pitch	Pitch compatibility
c_k, α_0, c_s, N	Eq. (11)	Avoidance of tip pointing
c_f,c_c, α_0, N	Eq. (14)	Avoidance of undercutting
c_f,c_c, α_0,c_s	Eq. (23)	Cutter shape coupling/limitation
c_s, α_C, N	Eq. (34)	Avoidance of thickness-wise interference (backlash)
c_f,c_k (c_{feqv})	Eq. (49)	Avoidance of radial interference
c_f,c_k (c_{feqv}), c_c, α_0, N	Eqs. (43)–(45)	Avoidance of corner contact and penetration

5.2.4. Addendum (c_k)

With increasing the addendum, the number of simultaneously meshing teeth and the contact ratio can be increased, which can result in decreasing the operating transmission error and noise; long addendum gears are typically used to obtain transverse contact ratio of two or above (which is particularly useful in e.g. automotive spur gears). Contact ratio-induced load sharing and resulting gear tooth strength can also be regulated by judicious choice of addendum.

Other considerations include:

- The whole depth required to accommodate a long addendum is bigger, resulting in lower attainable stiffness per tooth.
- Long addendum pinion with short addendum gear pairs are in some cases utilised to strengthen the pinion and adjusting the tip sliding velocities [2]

5.2.5. Dedendum (c_f)

Addendum and dedendum together define the tooth whole depth and are such closely coupled with regard to geometrical compatibility and interference. The following considerations apply:

- Increasing the tooth whole depth to achieve higher contact ratio can reduce the load carrying capacity of individual teeth
- On the other hand, for high contact ratio spur gears (above two), where one expects the load-sharing between mating teeth to compensate for this reduction, a small pitch error or other error could neutralise this effect, making high contact ratio designs applicable only under precise accuracy (and cost) conditions
- With increasing dedendum coefficient the leverage of the applied load increases therefore leading to higher fillet stress values

5.2.6. Profile shifting

Profile shifting simultaneously affects the apparent addendum, dedendum, tooth thickness and pressure angle. As such, it can be modelled equivalently by means of these other parameters.

5.2.7. Tooth thickness (c_s)

Tooth thickness has a direct effect on the tooth root cross-section and corresponding bending stresses and strength, with higher thickness giving better results. However, the geometrical compatibility of mating gears imposes limits on the thickness of mating teeth, or interference will occur. Backlash can be controlled for a given centre distance by controlling the thickness of the mating gear teeth. Other applicable design considerations are that:

- Pinion tooth thicknesses are often increased at the expense of the mating gear to strengthen the pinion [2].
- The determination of tooth thickness depends on the amount of desired backlash and the desired addendum, for a minimum size of tooth top land [2]. The choice of tooth thickness can be used to mitigate tooth pointing.

5.2.8. Number of teeth (N)

The numbers of teeth of two mating gears combined dictate their transmission ratio and basic kinematics. Almost all other characteristics of the gear pair, including contact ratio, load sharing, strength etc are implicitly affected by this choice. The number of teeth of a gear together with its module dictate the gear size.

5.3. Generalised model

Base on the explanation in Section 5.1, it can be concluded that the dependent design parameters can be reduced to independent design degree of freedoms only.

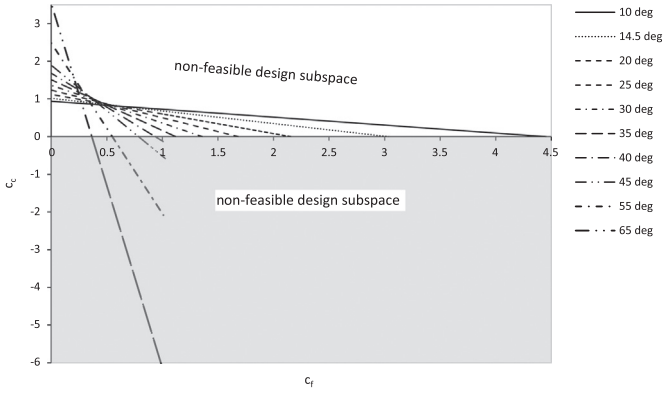

Fig. 10. Influence of pressure angle on manufacturing feasibility with given amount of tooth thickness.

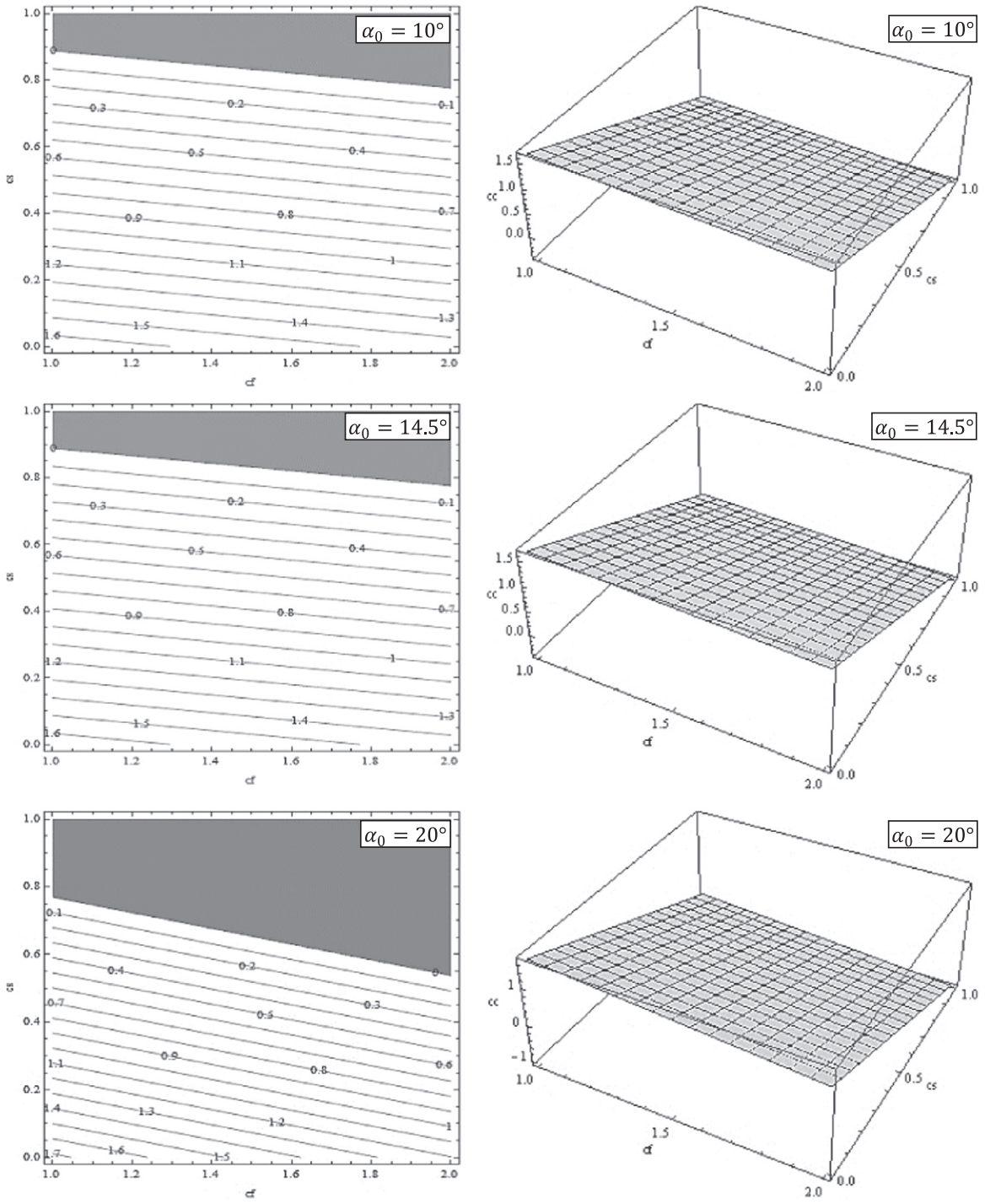

Fig. 11. Feasibility of a gear design according to Eq. (23) (relation between c_f, c_c, c_s and α_0),.

The design parameters that we discuss in this work are as: the number of teeth for gear 1 and 2, pressure angle, cutter tip radius, dedendum, addendum, tooth thickness.

With different formulations as explained in pervious sections, some of the design parameters are coupled and can be found from other formulations to be independent. Table 2 shows that how to use different formulas to reduce the design DOFs.

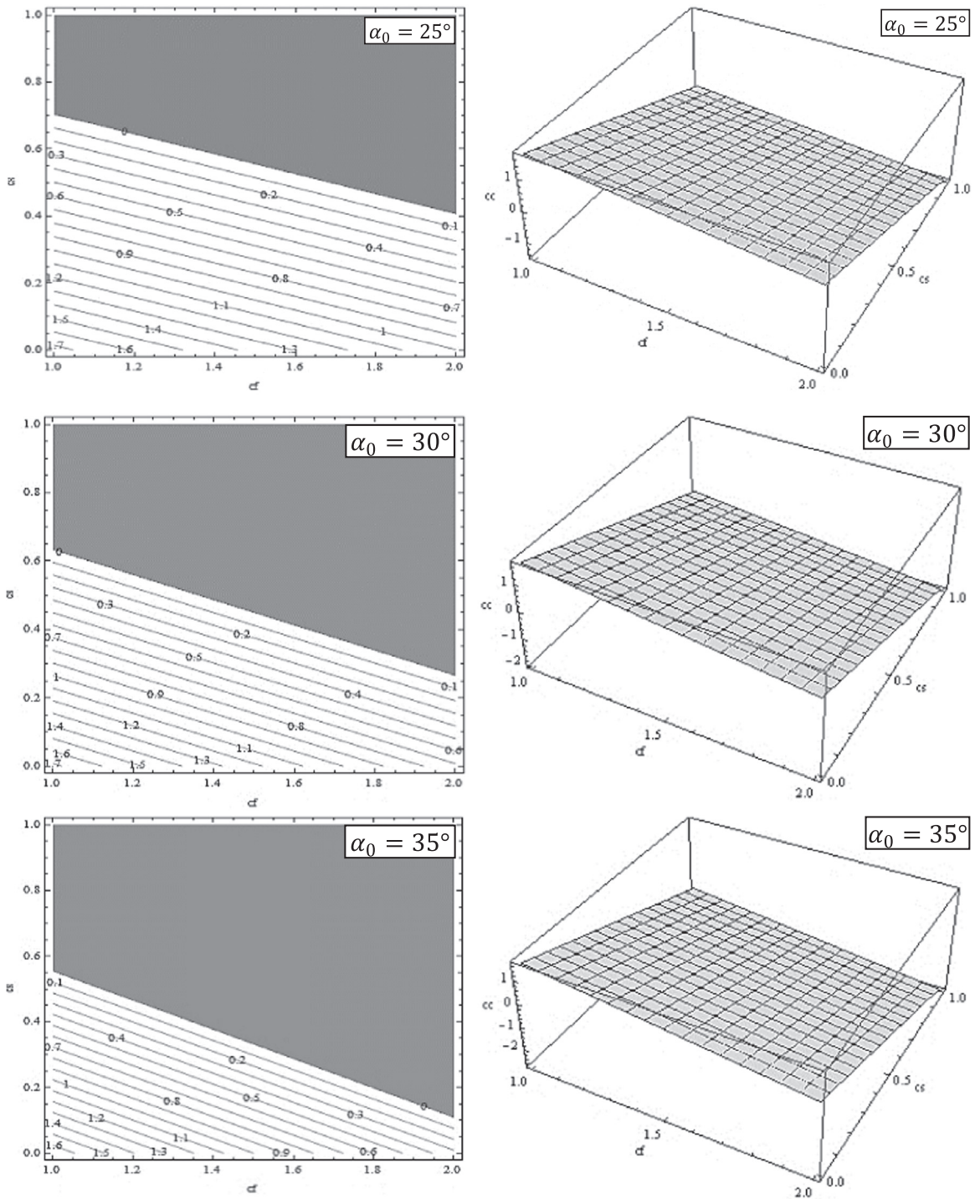

Fig. 11. (*continued*)

6. Results and discussion

6.1. Multi-parametric gear design maps and limit curves

Considering a pair of mating gears 1 and 2, in this section the relations between the design parameters such as the number of teeth for gear 1 and 2, pressure angle, cutter tip radius, dedendum, addendum, tooth thickness with regard to manufacturing feasibility (tip pointing/ non-pointing and undercutting/non-undercutting) and geometrical compatibility (interference/ non-

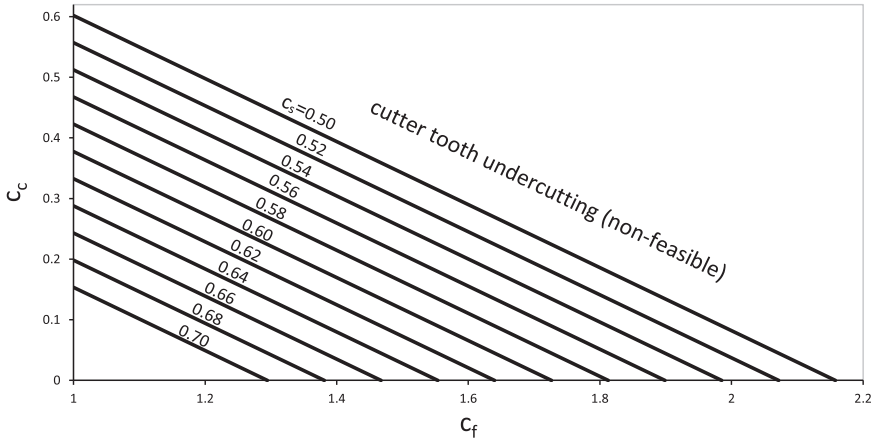

Fig. 12. The limitation of c_c-c_f combination for different values of tooth thickness coefficient.

interference) are discussed. The corresponding design subspaces and limit curves are identified.

6.1.1. Influence of pressure angle on manufacturability

Fig. 10 shows the manufacturing feasibility design space, according to Eq. (23), for different values of the pressure angle (10°, 14.5°, 20°, 25°, 30°, 35°, 40°, 45°, 50°, 60°) while the value of tooth thickness coefficient is given (c_s=0. 5). With increasing the pressure angle, the possibility of using larger c_f will be increased and simultaneously the possibility of using larger cutter tip radius will be decreased.

Fig. 11 reports the result of a more general study, according to Eq. (23), showing the complete relation between c_f, c_c, c_s and α_0 (10°, 14.5°, 20°, 25°, 30°, 35°).

In the left column, the diagonal lines present the amount of cutter tip radius coefficient (c_c) and the grey subspace corresponds to manufacturing non-feasibility. With smaller pressure angle, the feasible subspace will be bigger.

In the right column, a 3D plot is given of the relation between c_f, c_c, c_s for given amount of pressure angle. The subspace above the surface corresponds to non-feasible parameter combinations. With increasing the pressure angle, the feasible design space will be decreased.

6.1.2. Tooth thickness limitation (cutter tooth undercutting)

Eq. (23) presents the maximum value of c_c, with changing the amount of c_f while the value of c_s is given. In Eq. (23), different values for tooth thickness (c_s=0.50, 0.52, 0.54, 0.56, 0.58, 0.60, 0.62, 0.64, 0.66, 0.68, 0.70) present some limitations for different combinations of c_c and c_f. Fig. 12 presents the feasible design space for different $c_c - c_f$ combinations with regard to the limitation of tooth thickness. It is obvious that the tolerance area for different values of c_c, c_f will be decreased with increasing th value of tooth thickness,

6.1.3. Interference limits in the design space

Fig. 13 presents the limits to the design space imposed by interference for different combinations of the design parameters including N_1, N_2 (5, 10, 20, 40, 80), c_c, c_f, α_0 (10°, 14.5°, 20°, 25°, 30°, 35°. With regard to feasibility, Eq. (23) has been applied to find the maximum possible amount of tooth thickness coefficient. For calculating the interference subspace and corresponding limit curve the algorithm of corner contact and penetration method (Section 4.4) has been implemented. Above the tooth thickness limitation line lies non-feasible design space. The non-interference subspace is bounded from the left by the family of curves depending on the pressure angle and the number of teeth of the mating gear.

With increasing pressure angle and the number of teeth for gear 2, the design subspace corresponding to manufacturing feasibility and non-interference will be smaller. Hence larger gears with bigger pressure angle are more at risk of manufacturing and interference problems.

6.1.4. Undercutting limitation

Using Eq. (14) for different numbers of teeth for gear 1 (N_1=5, 10, 20, 40, 80) allows to design a gear without undercut as shown in Fig. 14, where the negative values for c_c are obviously not feasible. With increasing the number of gear teeth and the value of c_f, the safety of the design against undercutting will be increased. Increasing the pressure angle also enlarges the design subspace that is free from undercutting.

6.1.5. From radius limitation

Fig. 15 shows the form radius for a 20-tooth pinion for an exhaustive array of dedendum and cutter tip radius combinations for undercut and non-undercut root tooth as calculated by Eqs. (44) and (45). Extreme combinations of dedendum and cutter tip radii that are impossible to attain have been filtered out by use of Eq. (14) and therefore no corresponding values exist at the far end of the

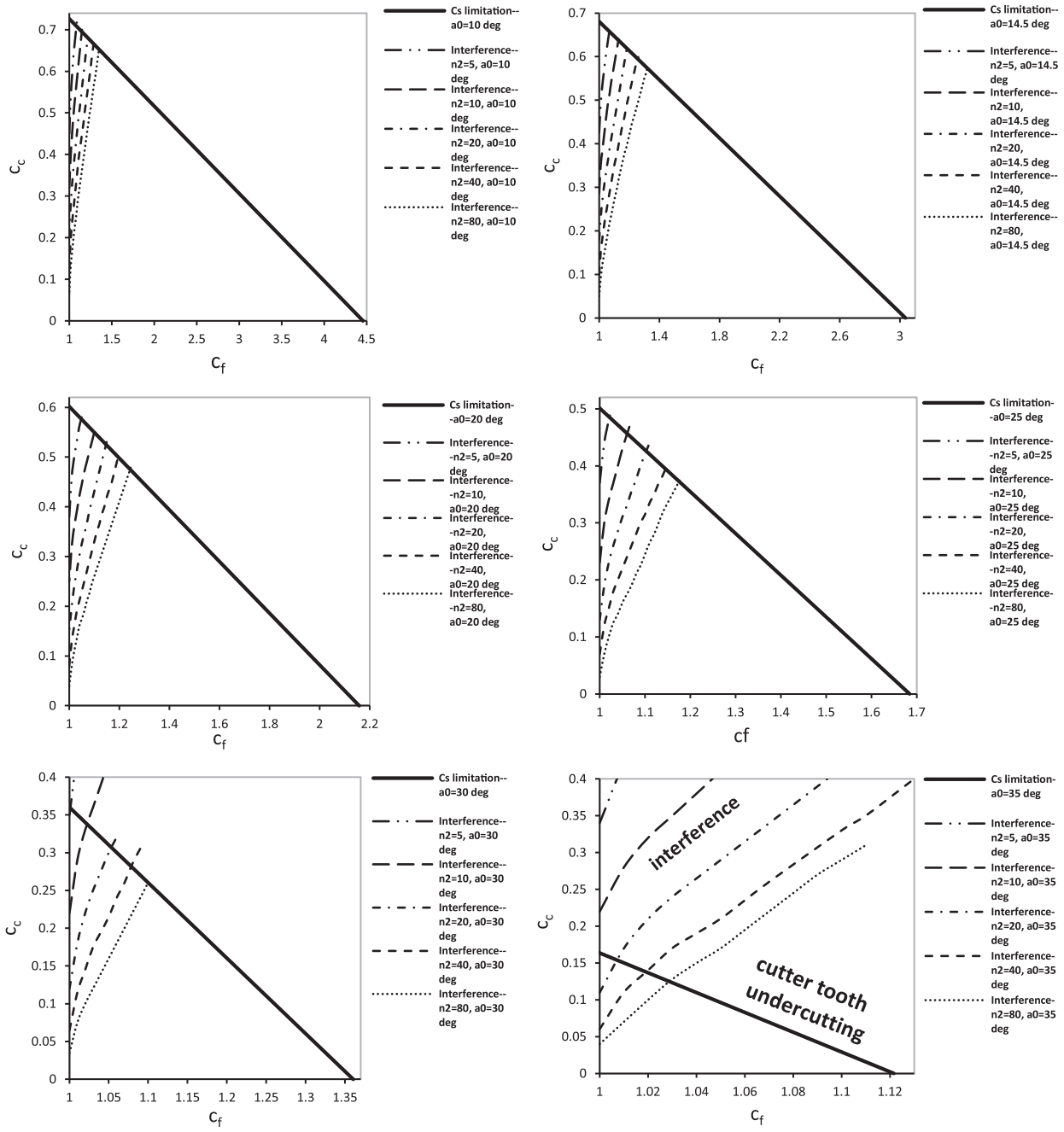

Fig. 13. The design subspace corresponding to manufacturability and non-interference for different combinations of the design parameters including N_1, N_2, c_{c1}, c_{f1}, and α_0.

chart, which is shown in Fig. 16.

It is easy to identify a region of dedendum and cutter tip radius combinations (Fig. 16), where the form radius is minimised and therefore the involute potion of the teeth is maximised. From Fig. 16 two different trends can be identified:

a) The form radius will be increased with combinations of large dedendum and small cutter tip radius (risk of undercutting will be increased)
b) The form radius can be increased also with combinations of small dedendum and large cutter tip radius (risk of interference will be increased)

As this is the region that produces the shallowest teeth with the stronger fillets, it is expected that this is the region where the

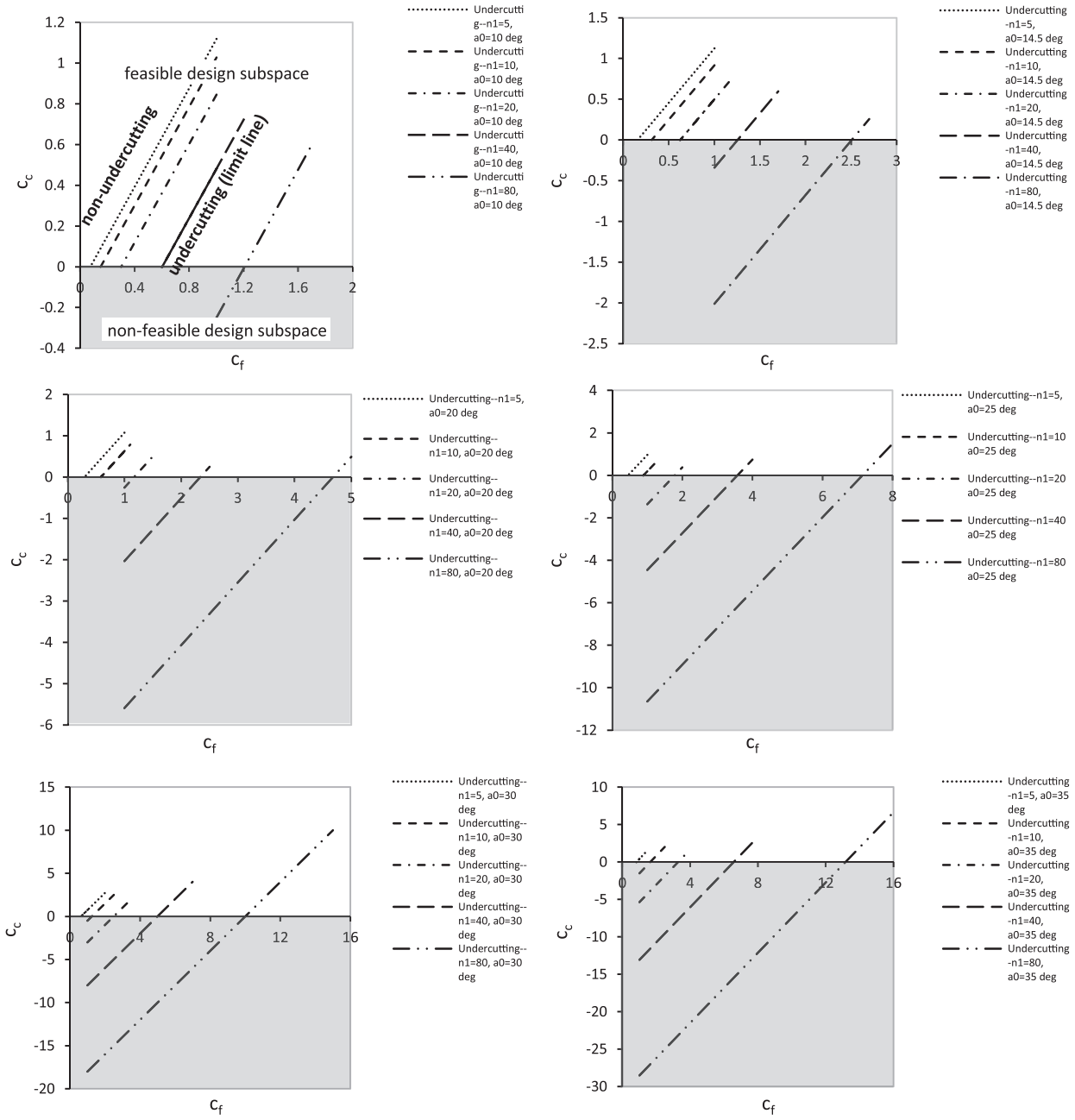

Fig. 14. Undercutting and non-undercutting design subspaces for different combinations of N_1, c_c, c_f,α_0. The grey subspace corresponds to non-feasible designs.

optimal designs are to be sought.

It is also important to note that the iso-r_s curves are linear throughout the definition field; this means that any increase of cutter tip radius must be made at the expense of increasing the dedendum coefficient by an analogous amount. The ratio of this analogy is easily determined from Eq. (26) as:

$$\frac{\Delta c_f}{\Delta c_c} = \frac{\cos\alpha_0}{\tan(45^0 + \frac{\alpha_0}{2})} \tag{47}$$

For the 20° gears studied here, this means that $\Delta c_f/\Delta c_c$=0. 658.

6.1.6. Addendum limitation

From Section 4.5 it can be concluded that instead of c_{f1}, we can use $c_{f1equivalent}$ as defined in Eq. (28), thereby incorporating the

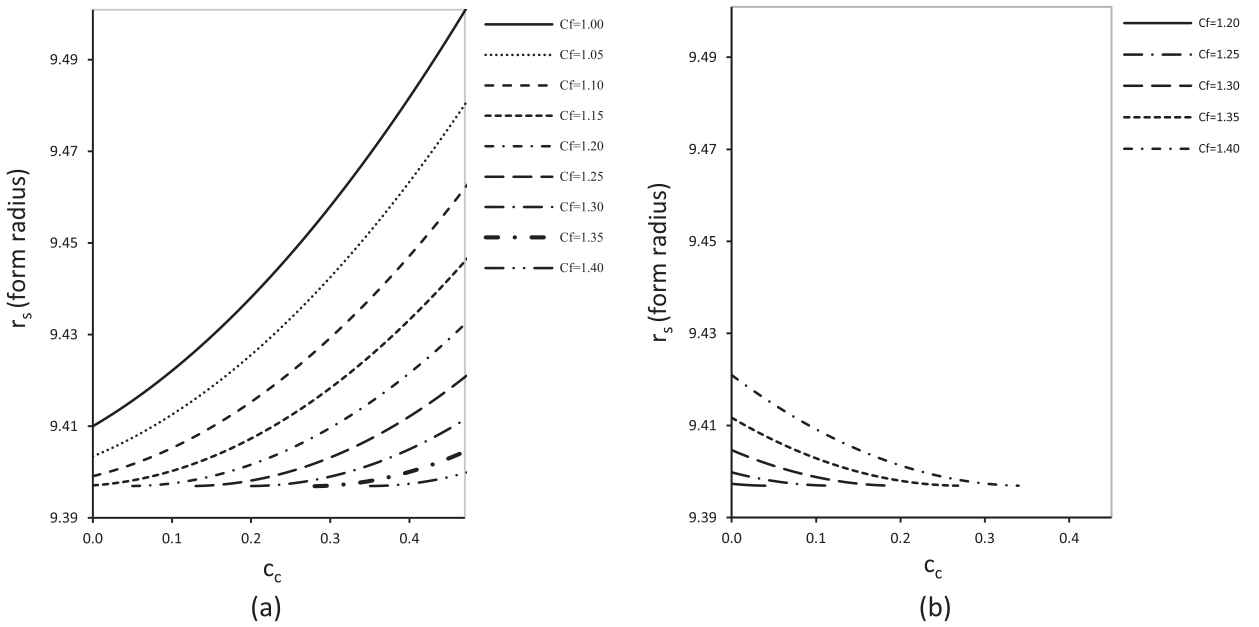

Fig. 15. Form radius limitation for (a) non-undercut and (b) undercut root tooth (N=20).

effect of the addendum in this new metric, which is always positive, since the addendum of the mating gear may not be larger than the dedendum of the reference gear. Fig. 17 presents the interference limit curve calculations in consideration of N_1, N_2, c_{c1}, c_{f1} and c_{k2}.

These results show that the risk of interference will be increased with using smaller value of c_{f1eqv}, which can be the result of increasing the addendum of the mating gear, and/ or bigger value of c_c.

The results show that the interference limit is not dependent on the number of teeth of gear 1 or the contact ratio, but only on the number of teeth of gear 2. Thus any combination of N_1, i_{12}, where $N_1 i_{12} = N_2$ is constant, produces an identical interference limit curve. This insight and in additional $c_{f1equivalent}$ allow reducing by two the dimensions of the parametric space, without loss of generality.

Considering the dedendum coefficient fixed, another relevant observation is that the contact ratio of will be increased with decreasing the amount of equivalent dedendum coefficient, which is practically equivalent to increasing the addendum coefficient of the mating gear and is not affected by the dedendum or the cutter tip radius of the reference gear, as shown in Fig. 18. The overall contact ratio will depend of course on the addenda (or equivalent dedenda) of both gears.

6.2. Compact and high contact ratio tooth forms

In Section 6.1 a large family of combinable plots has been presented, from which the manufacturability and compatibility design subspaces can be delimited.

Compact tooth form can be designed with minimising the total volume of gear tooth. Besides reducing the module, this can be done by reducing the number of teeth and minimising the clearance between gear teeth [126–131]. Higher pressure angles, which

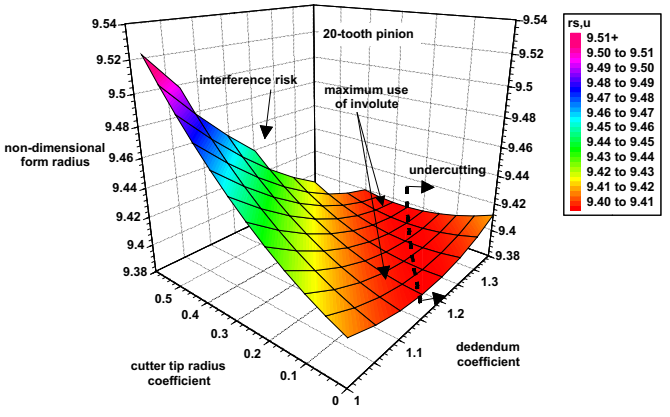

Fig. 16. Calculated non-dimensional form radius for a 20-tooth pinion for the possible combinations of dedendum and cutter tip radius. Useful designs lie between the rightmost (undercutting) and leftmost (interference) extremes.

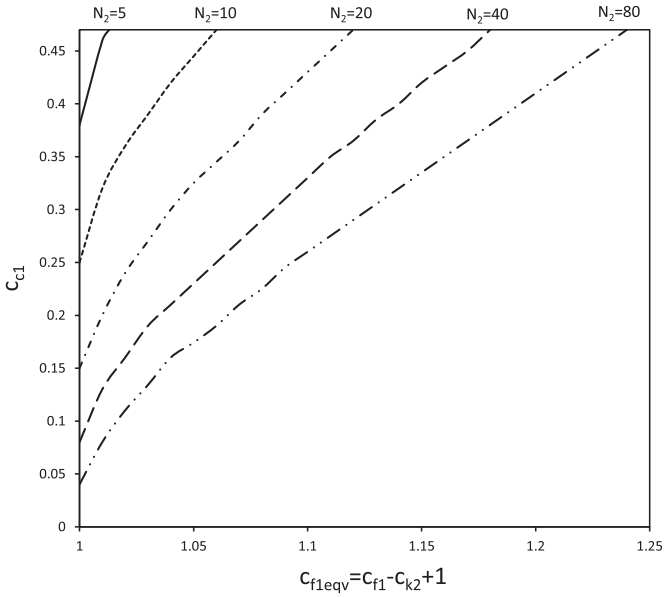

Fig. 17. Reducing the five-parametric design space for interference limit curves to the three-parametric design space c_{f1eqv}, c_{c1}, N_2 after elimination of parameters N_1, i_{12} and c_{k2}.

are conductive to higher load carrying capacity and small modules and addenda, which are conductive to high scoring/ scuffing resistance, can also be chosen.

Likewise, while only pressure angle and the addenda of both gears affect the contact ratio, their feasible values when attempting to increase the contact ratio are affected by many other design parameters (including the limitation of form radius). The produced design spaces allows a fast assessment of these limits and corresponding attainable values.

Given that the design space, considering both gears in a pair, contains multiple parameters and the design goals vary from one application to another, from the provided analytical mapping of the design space limits the optimal (or Pareto-optimal) solutions can be found on a case by case basis. Fig. 19 offers a qualitative summary of several of the plots presented in Section 6.1 and can serve as a starting point and design guideline.

As the relations between the design parameters reduced to the independent design DOFs, selecting the design parameters can be easy and fast to find compact and/ or high contact ratio tooth forms.

Already, in high performance gear applications in the automotive and aerospace sectors the industry has moved away from the standard tooth proportions and many gear designs currently being developed or in use fall in the regions of the design space denoted by the thick arrows (left and top left part of the feasible design space). This is still largely based on trial-and-error. To the best knowledge of the authors, Fig. 19 is the first representation to explain why such designs are optimal in the c_f-c_c space, in terms of compactness and contact ratio (both of which are a function of c_{feqv}) allowing a better-informed design space exploration and design optimisation.

6.3. Implications of the choice of pressure angle

According to the results of Section 6.1.2, the pressure angle plays an important role regarding not only gear performance, but also the size/extent of the design subspace that is consistent with manufacturability and compatibility. Larger pressure angles are

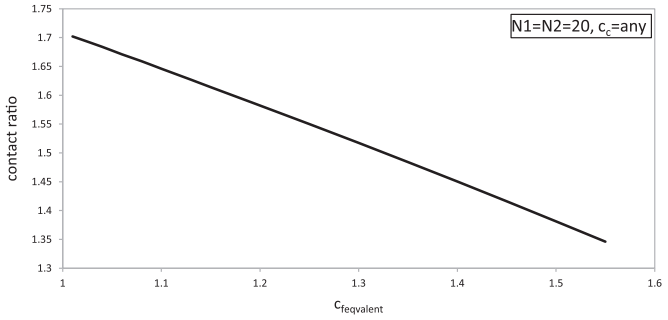

Fig. 18. The relation between equivalent dedendum coefficient (c_{feqv}) and gear contact ratio.

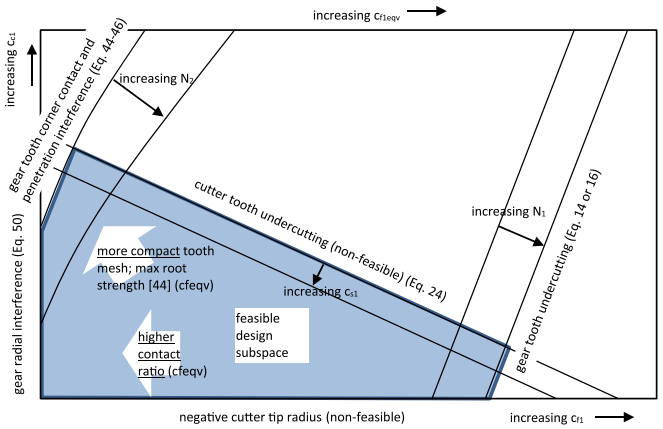

Fig. 19. Overlay of different limit lines and delineation of feasible and non-feasible design subspaces on the multi-parametric non-dimensional design space (c_f/c_{feqv}, c_c, c_s, N). The limit lines corresponding to different values of a_0 are not shown for clarity.

only feasible within limited design subspaces.

This means that for the large pressure angles that are used for special applications such as high capacity load carrying in heavy industry, the presented mapping can be used to precisely navigate the narrow design space in order to reach feasible designs.

7. Conclusion

This paper presented a number of original and reworked mathematical models that are relevant to assessing the manufacturability and geometrical compatibility of gears, considering the multi-dimensional design space involving simultaneously the pressure angle, module, addendum, dedendum, cutter tip radius, thickness, and number of teeth of both gears in a pair. These models were synthesised into one comprehensive meta-model that supports fast assessment of gear design feasibility.

Various modes of interference were considered as well as the manufacturability of the individual gear teeth in terms of pointing and undercutting. Differences between different available models (e.g. with regard to undercutting were identified and discussed). Furthermore, models for pitch compatibility and corner contact and penetration were presented that provide new possibilities for non-standard and compact tooth form designs.

The resulting combined model serves to provide a complete analytical overview of the multi-parametric design space and is suitable for the fast assessment of existing designs, for implicit or explicit (direct) gear design, for extracting design guidelines, and for design optimisation. The model can be used to identify and explore highly promising under-used subspaces of the parametric design space, which are currently of significant interest to i.e. the automotive and aerospace industries.

References

[1] F.L. Litvin, Gear Geometry and Applied Theory, *Prentice Hall*, 1994.
[2] D.P. Townsend, Dudley's Gear Handbook, *McGraw Hill*, 1992.
[3] E. Buckingham, Analytical Mechanics of Gears, *Dover Publications Inc*, 1988.
[4] M.F. Spotts, Design of Machine Elements, 6nd Edition, *Prentice hall*, Englewood Cliffs, 1985.
[5] H.E. Merritt, Gears, 3rd Edition, *Isaac Pitman & Sons*, 1954.
[6] G.M. Maitra, Handbook of Gear Design, *Tata McGraw-Hill Education*, New Delhi, 2001.
[7] S. Prabhakaran, S. Ramachandran, Comparison of bending stress of a spur gear for different materials and modules using AGMA standards in FEA, Adv. Mater. Res. 739 (2013) 382–387.
[8] A. KISSsoft, version 03/2011, 2011.
[9] HyGEARS, Involute Simulation Software Inc., Version 4.0, 2014.
[10] Gear Design Pro, Dontyne System, version 4.5, 2011.
[11] GearTeq, Camnetics Incorporated, version 20.32.341, 2012.
[12] Geartrax, Camnetics Incorporated, version 20.671 for SolidWorks 2012, 2012.
[13] T. Nonaka, D. Satoh, K. Miyake, A. Kubo, Strength of spur gear teeth with small modules of the order of 0.1 mm: (1st report, nature of tooth failure), *Nippon Kikai Gakkai Ronbunshu, C Hen/Transactions of the Japan Society of Mechanical Engineers*, Part C, 68, 8, 2431, –2437, 2002.
[14] S. Baglioni, F. Cianetti, L. Landi, Influence of the addendum modification on spur gear efficiency, Mech. Mach. Theory 49 (2012) 216–233.
[15] S. Li, Effect of addendum on contact strength, bending strength and basic performance parameters of a pair of spur gears, Mech. Mach. Theory 43 (12) (2008) 1557–1584.
[16] V. Balambica, T.J. Prabhu, R. VenkateshBabu, E.V. Deepak, Design and static analysis of an addendum modified helical gear tooth, Appl. Mech. Mater. 391 (2013) 132–138.
[17] T. Chen, W. Sun, X. Zhang, An analytical method to determine the addendum modification parameters of involute helical gears, Proc. Inst. Mech. Eng. C: J. Mech. Eng. Sci. 225 (11) (2011) 2516–2524.
[18] V. Atanasiu, M.R. Iacob, Tooth wear effects on dynamic transmission error of spur gears with addendum modifications, Int. Rev. Mech. Eng. 4 (6) (2010) 638–644.
[19] T.A. Antal, A new algorithm for helical gear design with addendum modification, Mechanika 77 (3) (2009) 53–57.
[20] H. Imrek, A. Unuvar, Investigation of influence of load and velocity on scoring of addendum modified gear tooth profiles, Mech. Mach. Theory 44 (5) (2009) 938–948.
[21] M.A.S. Arikan, Determination of addendum modification coefficients for spur gears operating at non-standard center distances, ASME Int. Des. Eng. Tech. Conf. Comput. Inf. Eng. Conf. 4 (2003) 489–499.

[22] J.I. Pedrero, M. Artés, Approximate equation for the addendum modification factors for tooth gears with balanced specific sliding, Mech. Mach. Theory 31 (7) (1996) 925–935.
[23] P.D. Rockwell, Profile shift in external parallel-axis cylindrical involute gears, Gear Technol. 18 (6) (2001) 18–25.
[24] C. Wang, H. Liu, C. -L. Xiang, Influences of profile modification on dynamic characteristics of involute spur gears under a fluctuating torque, Zhendong yu Chongji/J. Vib. Shock 33 (24) (2014) 32–38.
[25] S. Barone, L. Borgianni, P. Forte, Evaluation of the effect of misalignment and profile modification in face gear drive by a finite element meshing simulation, ASME J. Mech. Des. 126 (5) (2004) 916–924.
[26] Z. Chen, Y. Shao, Mesh stiffness calculation of a spur gear pair with tooth profile modification and tooth root crack, Mech. Mach. Theory 62 (2013) 63–74.
[27] G. Bonori, M. Barbieri, F. Pellicano, Optimum profile modifications of spur gears by means of genetic algorithms, J. Sound Vib. 313 (3–5) (2008) 603–616.
[28] H.H. Lin, F.B. Oswald, D.P. Townsend, Dynamic loading of spur gears with linear or parabolic tooth profile modifications, Mech. Mach. Theory 29 (8) (1994) 1115–1129.
[29] S. Sankar, M. Nataraj, Profile modification-a design approach for increasing the tooth strength in spur gear, Int. J. Adv. Manuf. Technol. 55 (1) (2001) 1–10.
[30] R.-H. Hsu, H.-H. Su, Tooth contact analysis for helical gear pairs generated by a modified hob with variable tooth thickness, Mech. Mach. Theory 71 (2014) 40–51.
[31] K.J. Sharif, H.P. Evans, R.W. Snidle, Wear modelling in worm gears, Solid Mech. Appl. 134 (2006) 371–383.
[32] F.L. Litvin, C.-L. Hsiao, M.D. Ziskind, Computerized overwire (ball) measurement of tooth thickness of worms, screws and gears, Mech. Mach. Theory 33 (6) (1998) 851–877.
[33] S. Li, A. Kahraman, Prediction of spur gear mechanical power losses using a transient elastohydrodynamic lubrication model, Tribology Trans. 53 (4) (2010) 554–563.
[34] B.R. Höhn, P. Oster, U. Schrade, Studies on the micropitting resistance of case-carburised gears - Industrial application of the new calculation method, VDI-Berichte (2005) 1287–1307.
[35] F.M. Khoshnaw, N.M. Ahmed, Effect of the load location along the involute curve of spur gears on the applied stress at the fillet radius, Mater. und Werkst. 39 (6) (2008) 407–414.
[36] A.L. Kapelevich, R.E. Kleiss, Direct gear design for spur and helical involute gears, Gear Technol. 19 (5) (2002) 29–35.
[37] Y. Hu, X.-C. Zhang, Z.-J. Yang, J. Zhang, Precision cutting of spiral bevel gear with spherical involute tooth profile, Beijing Gongye Daxue Xuebao / J. Beijing Univ. Technol. 37 (5) (2011) 641–647.
[38] F. Jarchow, Q.J. Yang, Operational reliability of gear units with special consideration of the dedendum capacity, Antriebstechnik 29 (1990) 44–47.
[39] A. Sanders, D.R. Houser, A. Kahraman, J. Harianto, S. Shon, An experimental investigation of the effect of tooth asymmetry and tooth root shape on root stresses and single tooth bending fatigue life of gear teeth, ASME Int. Des. Eng. Tech. Conf. Comput. Inf. Eng. Conf. 8 (2011) 297–305.
[40] Th Costopoulos, V. Spitas, Reduction of gear fillet stresses by using one-sided involute asymmetric teeth, Mech. Mach. Theory 44 (8) (2009) 1524–1534.
[41] N. Chaphalkar, G. Hyatt, N. Bylund, Analysis of gear root forms: a review of designs, standards and manufacturing methods for root forms in cylindrical gears, AGMA Fall Tech. Meet. (2013) 33–39.
[42] F.W. Brown, S.R. Davidson, D.B. Hanes, D.J. Weires, A. Kapelevich, Analysis and testing of gears with asymmetric involute tooth form and optimized fillet form for potential application in helicopter main drives, AGMA Fall Tech. Meet. (2010) 172–186.
[43] C. Spitas, V. Spitas, A. Amani, Multi-parametric investigation of interference in non-standard spur gear teeth, Mech. Mach. Theory 88 (2015) 105–124.
[44] C. Spitas, V. Spitas, A. Amani, M. Rajabalinejad, Parametric investigation of the combined effect of whole depth and cutter tip radius on the bending strength of 20 involute gear teeth, Acta Mech. 225 (2) (2014) 361–371.
[45] C. Spitas, V. Spitas, A FEM study of the bending strength of circular fillet gear teeth compared to trochoidal fillets produced with enlarged cutter tip radius, Mech. Based Des. Struct. Mach. 35 (1) (2007) 59–73.
[46] R. Thirumurugan, G. Muthuveerappan, Maximum fillet stress analysis based on load sharing in normal contact ratio spur gear drives, Mech. Based Des. Struct. Mach. 38 (2) (2010) 204–226.
[47] P. Marimuthu, G. Muthuveerappan, Influence of pressure angle on load sharing based stresses in asymmetric normal contact ratio spur gear drives, Appl. Mech. Mater. 465–466 (2014) 1229–1233.
[48] J. Xiao, X.L. Deng, J.N. He, W.X. Ma, Y. Li, J.S. Li, Simulation and analysis about different pressure angle in involute gears based on neural network, Appl. Mech. Mater. 540 (2014) 88–91.
[49] A. Sandooja, S. Jadhav, Analysis of gear geometry and durability with asymmetric pressure angle, SAE Int. J. Commer. Veh. 5 (2) (2012) 546–558.
[50] W. Kim, J.Y. Lee, J. Chung, Dynamic analysis for a planetary gear with time-varying pressure angles and contact ratios, J. Sound Vib. 331 (4) (2012) 883–901.
[51] F.M. Khoshnaw, N.M. Ahmed, The pressure angle effects of spur gears on stress concentration factor, Eng. Comput. 26 (4) (2009) 360–374.
[52] G.A. Danieli, Analytical description of meshing of constant pressure angle teeth profiles on a variable radius gear and its applications, ASME J. Mech. Des. 122 (1) (2000) 123–129.
[53] J. Lin, A pressure angle function method for describing tooth profiles of planar gears, ASME J. Mech. Des. 131 (5) (2009) 0510051–0510058.
[54] C. Spitas, V. Spitas, Effect of cutter pressure angle on the undercutting risk and bending strength of 20° involute pinions cut with equivalent nonstandard cutters, Mech. Based Des. Struct. Mach. 36 (2) (2008) 189–211.
[55] V.I. Medvedev, A.E. Volkov, M.A. Volosova, O.E. Zubelevich, Mathematical model and algorithm for contact stress analysis of gears with multi-pair contact, Mech. Mach. Theory 86 (2015) 156–171.
[56] Y. -C. Chen, C. -C. Lo, Contact stress and transmission errors under load of a modified curvilinear gear set based on finite element analysis, Proc. Inst. Mech. Eng. C: J. Mech. Eng. Sci. 229 (2) (2015) 191–204.
[57] B. Chen, D. Liang, Y. Gao, Geometry design and mathematical model of a new kind of gear transmission with circular arc tooth profiles based on curve contact analysis, Proc. Inst. Mech. Eng. C: J. Mech. Eng. Sci. 228 (17) (2014) 3200–3208.
[58] R. -H. Hsu, H. -H. Su, Tooth contact analysis for helical gear pairs generated by a modified hob with variable tooth thickness, Mech. Mach. Theory 71 (2014) 40–51.
[59] I. Tsuji, K. Kawasaki, H. Gunbara, H. Houjoh, S. Matsumura, Tooth contact analysis and manufacture on multitasking machine of large-sized straight bevel gears with equi-depth teeth, ASME J. Mech. Des. 135 (3) (2013) (ID:34504).
[60] C. Spitas, V. Spitas, Fast unconditionally stable 2-D analysis of non-conjugate gear contacts using an explicit formulation of the meshing equations, Mech. Mach. Theory 46 (7) (2011) 869–879.
[61] M. Kolivand, A. Kahraman, An ease-off based method for loaded tooth contact analysis of hypoid gears having local and global surface deviations, ASME J. Mech. Des. 132 (7) (2010) 0710041–0710048.
[62] S. Li, Finite element analyses for contact strength and bending strength of a pair of spur gears with machining errors, assembly errors and tooth modifications, Mech. Mach. Theory 42 (1) (2007) 88–114.
[63] S. -C. Hwang, J. -H. Lee, D. -H. Lee, S. -H. Han, K. -H. Lee, Contact stress analysis for a pair of mating gears, Math. Comput. Model. 57 (1-2) (2013) 40–49.
[64] R. Imin, M. Geni, Stress analysis of gear meshing impact based on SPH method, Math. Probl. Eng. (2014) (ID: 328216).
[65] S. Naidoo Lingamanaik, B.K. Chen, P. Palanisamy, Finite element analysis on the formation and distribution of residual stresses during quenching of low carbon bainitic-martensitic large gears, Comput. Mater. Sci. 79 (2013) 627–633.
[66] S. Wang, G.R. Liu, G.Y. Zhang, L. Chen, Design of asymmetric gear and accurate bending stress analysis using the es-pim with triangular mesh, Int. J. Comput. Methods 8 (4) (2011) 759–772.
[67] H. Gao, Z. Li, Z. Deng, Sensitivity analysis of cup-shaped flexible gear parameters to its stress based on ANSYS, Jixie Gongcheng Xuebao/J. Mech. Eng. 46 (5) (2010) 1–7.
[68] R. Thirumurugan, G. Muthuveerappan, Maximum fillet stress analysis based on load sharing in normal contact ratio spur gear drives, Mech. Based Des. Struct. Mach. 38 (2) (2010) 204–226.
[69] A.R. Hassan, Contact stress analysis of spur gear teeth pair, World Acad. Sci., Eng. Technol. 58 (2009) 611–616.
[70] F.L. Litvin, D. Vecchiato, E. Gurovich, A. Fuentes, I. Gonzalez-Perez, K. Hayasaka, K. Yukishima, Computerized developments in design, generation, simulation of meshing, and stress analysis of gear drives, Meccanica 40 (3) (2005) 291–323.
[71] Y. -C. Chen, C. -B. Tsay, Stress analysis of a helical gear set with localized bearing contact, Finite Elem. Anal. Des. 38 (8) (2002) 707–723.
[72] C.K. Tan, P. Irving, D. Mba, A comparative experimental study on the diagnostic and prognostic capabilities of acoustics emission, vibration and spectrometric

oil analysis for spur gears, Mech. Syst. Signal Process. 21 (1) (2007) 208–233.
[73] Y. Cai, T. Hayashi, Linear approximated equation of vibration of a pair of spur gears (theory and experiment), ASME J. Mech. Des. 116 (2) (1994) 558–564.
[74] O.D. Mohammed, M. Rantatalo, J. -O. Aidanpää, Dynamic modelling of a one-stage spur gear system and vibration-based tooth crack detection analysis, Mech. Syst. Signal Process. 54 (2015) 293–305.
[75] A. Farshidianfar, A. Saghafi, Global bifurcation and chaos analysis in nonlinear vibration of spur gear systems, Nonlinear Dyn. 75 (4) (2014) 783–806.
[76] M. Divandari, B.H. Aghdam, R. Barzamini, Tooth profile modification and its effect on spur gear pair vibration in presence of localized tooth defect, J. Mech. 28 (2) (2012) 373–381.
[77] A. Spitas, Th. N. Costopoulos, V.A. Spitas, Calculation of transmission errors, actual path of contact and actual contact ratio of non-conjugate gears, VDI-Berichte 2 (1665) (2002) 981–994.
[78] C. Yurong, T. Hayashi, The estimation of vibration of a pair of spur gears due to their tooth profile errors. (2nd Report), The linear approximated formula of vibration in case of each contact ratio, Seimitsu Kogaku Kaishi/J. Jpn. Soc. Precis. Eng. 57 (2) (1991) 273–279.
[79] C. Spitas, V. Spitas, Calculation of overloads induced by indexing errors in spur gearboxes using multi-degree-of-freedom dynamical simulation, Proc. Inst. Mech. Eng. K: J. Multi-body Dyn. 220 (4) (2006) 273–282.
[80] R.G. Parker, S.M. Vijayakar, T. Imajo, Non-linear dynamic response of a spur gear pair: modelling and experimental comparisons, J. Sound Vib. 237 (3) (2000) 435–455.
[81] I. Howard, S. Jia, J. Wang, The dynamic modelling of a spur gear in mesh including friction and a crack, Mech. Syst. Signal Process. 15 (5) (2001) 831–853.
[82] H.N. Özgüven, A non-linear mathematical model for dynamic analysis of spur gears including shaft and bearing dynamics, J. Sound Vib. 145 (2) (1991) 239–260.
[83] M. Faggioni, F.S. Samani, G. Bertacchi, F. Pellicano, Dynamic optimization of spur gears, Mech. Mach. Theory 46 (4) (2011) 544–557.
[84] T. Osman, Ph Velex, Static and dynamic simulations of mild abrasive wear in wide-faced solid spur and helical gears, Mech. Mach. Theory 45 (6) (2010) 911–924.
[85] S. Li, A. Kahraman, A tribo-dynamic model of a spur gear pair, J. Sound Vib. 332 (20) (2013) 4963–4978.
[86] L. Walha, T. Fakhfakh, M. Haddar, Backlash effect on dynamic analysis of a two-stage spur gear system, J. Fail. Anal. Prev. 6 (3) (2006) 60–68.
[87] K.J. Huang, H.W. Wei, Approaches to parametric element constructions and dynamic analyses of spur/helical gears including modifications and undercutting, Finite Elem. Anal. Des. 46 (12) (2010) 1106–1113.
[88] M.T. Khabou, N. Bouchaala, F. Chaari, T. Fakhfakh, M. Haddar, Study of a spur gear dynamic behavior in transient regime, Mech. Syst. Signal Process. 25 (8) (2011) 3089–3101.
[89] F. Chaari, T. Fakhfakh, M. Haddar, Analytical modelling of spur gear tooth crack and influence on gear mesh stiffness, Eur. J. Mech. A/Solids 28 (3) (2009) 461–468.
[90] Z. Chen, Y. Shao, Dynamic simulation of spur gear with tooth root crack propagating along tooth width and crack depth, Eng. Fail. Anal. 18 (8) (2011) 2149–2164.
[91] Z. Chen, Y. Shao, Mesh stiffness calculation of a spur gear pair with tooth profile modification and tooth root crack, Mech. Mach. Theory 62 (2013) 63–74.
[92] Y. Pandya, A. Parey, Simulation of crack propagation in spur gear tooth for different gear parameter and its influence on mesh stiffness, Eng. Fail. Anal. 30 (2013) 124–137.
[93] R. Guilbault, S. Lalonde, M. Thomas, Modeling and monitoring of tooth fillet crack growth in dynamic simulation of spur gear set, J. Sound Vib. 343 (2015) 144–165.
[94] S. Li, A. Kahraman, A transient mixed elastohydrodynamic lubrication model for spur gear pairs, J. Tribology 132 (1) (2010) 1–9.
[95] Y. Wang, H. Li, J. Tong, P. Yang, Transient thermoelastohydrodynamic lubrication analysis of an involute spur gear, Tribology Int. 37 (10) (2004) 773–782.
[96] P. Kumar, P.K. Saini, P. Tandom, Transient elastohydrodynamic lubrication analysis of an involute spur gear using couple-stress fluid, Proc. Inst. Mech. Eng. J: J. Eng. Tribol. 221 (6) (2007) 743–754.
[97] Y. -Q. Wang, X. -J. Yi, Non-Newtonian transient thermoelastohydrodynamic lubrication analysis of an involute spur gear, Lubr. Sci. 22 (10) (2010) 465–478.
[98] M. Parsa, S. Akbarzadeh, A new load-sharing-based approach to model mixed-lubrication contact of spur gears, Proc. Inst. Mech. Eng. J: J. Eng. Tribol. 228 (11) (2014) 1319–1329.
[99] S. Li, A. Kahraman, M. Klein, A fatigue model for spur gear contacts operating under mixed elastohydrodynamic lubrication conditions, ASME J. Mech. Des. 134 (4) (2012) (ID: 041007).
[100] R. Larsson, Transient non-Newtonian elastohydrodynamic lubrication analysis of an involute spur gear, Wear 207 (1–2) (1997) 67–73.
[101] A. Amani, M. Rajabalinejad, C. Spitas, Modelling of elastohydrodynamic lubrication problems in gears, in: *Proceedings of the 22nd International Symposium on Transport Phenomena (ISTP22)*, Delft, Netherlands, 8 pages, 2011.
[102] A.L. Kapelevich, Direct Gear Design, CRC Press, *Taylor and Francis Group*, 2013.
[103] M. Rackov, M. Veres, Z. Kanovic, S. Kuzmanovic, HCR gearing and optimization of its geometry, Adv. Mater. Res. 633 (2013) 117–134.
[104] B. -W. Bair, Tooth profile generation and analysis of crowned elliptical gears, ASME, J. Mech. Des. 131 (7) (2009) 0745031–0745036.
[105] M.A.S. Arikan, Determination of addendum modification coefficients for spur gears operating at non-standard center distances, ASME 2003 Int. Des. Eng. Tech. Conf. Comput. Inf. Eng. Conf. 4 A (2003) 489–499.
[106] O. Alipiev, S. Antonov, T. Grozeva, Generalized model of undercutting of involute spur gears generated by rack-cutters, Mech. Mach. Theory 64 (2013) 39–52.
[107] J. He, W. Zhang, H. Zhang, W. Ma, S. Chen, Q. Li, Y. Gao, Study on minimum teeth without undercutting of standard involute gears, Adv. Mater. Res. 199–200 (2011) 329–336.
[108] J. Brauer, Analytical geometry of straight conical involute gears, Mech. Mech. Theory 37 (2002) 127–141.
[109] C. Spitas, V. Spitas, Direct analytical solution of a modified form of the meshing equations in two dimensions for non-conjugate gear contact, Appl. Math. Model. 32 (10) (2008) 2162–2171.
[110] C. Spitas, Th Costopoulos, V. Spitas, Direct analytical solution of the inverse gear tooth contact analysis problem, Inverse Probl. Sci. Eng. 16 (2) (2008) 171–186.
[111] E.B. Vulgakov, Theory of Involute Gears, Mashinostroenie, Moscow, 1995 (in Russian).
[112] C. Spitas, V. Spitas, Can non-standard involute gears of different modules mesh?, IMECE J. Mech. Eng. Sci. 220 (8) (2006) 1305–1313.
[113] GOST 13755-81, Basic requirements for interchangeability. Gearings cylindric evolvent gears. Basic rack, 1981.
[114] ISO 53, Cylindrical gears for general and heavy engineering- Standard basic rack tooth profile, 1974.
[115] NF E 23-011, Cylindrical gears for general and heavy engineering - Basic rack and modules (similar to ISO 467 and ISO 53), 1972.
[116] ISO/TR 4467, Addendum Modification of the Teeth of Cylindrical Gears for Speed-reducing and Speed Increasing Gear Pairs, 1982.
[117] JIS B 1702-72, Accuracy for Spur and Helical Gears, 1976.
[118] DIN 867, Basic Rack Tooth Profiles for Involute Teeth of Cylindrical Gears for General Engineering and Heavy Engineering, 1986.
[119] AGMA, 201.02 and 201.02A, Tooth Proportions for Coarse Pitch Involute Spur Gears, Gear Manufacturers Association (AGMA), Alexandria VA, 1968.
[120] DIN 3972, Reference Profiles of Gear-cutting Tools for Involute Tooth Systems according to DIN867, 1952.
[121] ANSI/AGMA 1006-A97, Tooth proportions for plastic gears, Appendix F "Generating Gear Geometry without Racks", 1997.
[122] AKGears, Gear Tooth Root Fillet Optimization Software, 2015.
[123] A. Amani, V. Spitas, C. Spitas, Influence of centre distance deviation on the interference of a spur gear pair, Int. J. Powertrains 4 (4) (2015) 315–337.
[124] V.N. Rubtsov, Radial interference when cutting gears with internal teeth by means of a cutter with a rounded tip, Russ. Eng. Res. 28 (11) (2008) 1151–1152.
[126] M. Savage, J.J. Coy, D.P. Townsend, Optimal tooth numbers for compact standard spur gear sets, ASME J. Mech. Des. 104 (4) (1982) 749–758.
[127] T. Nguyen, H.H. Lin, Compact design for non-standard spur gears, J. Mech. Aerosp. Ind. Eng. 2 (1) (2011) 1–15.
[128] J.W. Polder, H. Broekhuisen, Tip-fillet interference in cylindrical gears, ASME Des. Eng. Tech. Conf. Comput. Inf. Eng. Conf. 4A (2003) 473–479.
[129] J.D. Smith, Gear Noise and Vibration, second edition, Marcel Dekker Inc., New York Basel, 2003.
[130] R.E. Kleiss, Kapelevich, KleissJr., A.L., New Opportunities with Molded gears, *AGMA Fall Technical Meeting*, Detroit, October 3-5, (01FTM9), 2001.
[131] F.L. Litvin, D.H. Kim, Computerized design, generation and simulation of meshing of modified involute spur gears with localized bearing contact and reduced level of transmission errors, ASME J. Mech. Des. 119 (1997) 96–100.